การวิเคราะห์ทางทฤษฎีของเครื่องปฏิกรณ์เมมเบรนแบบหลายขั้น สำหรับปฏิกิริยาคู่ควบของมีเทนแบบออกซิเดชัน

นางสาวสิริกาญจน์ ติรเศรษฐ์

วิทยานิพนธ์นี้เป็นส่วนหนึ่งของการศึกษาตามหลักสูตรปริญญาวิศวกรรมศาสตรมหาบัณฑิต
สาขาวิชาวิศวกรรมเคมี ภาควิชาวิศวกรรมเคมี
คณะวิศวกรรมศาสตร์ จุฬาลงกรณ์มหาวิทยาลัย
ปีการศึกษา 2554

THEORETICAL ANALYSIS OF A MULTI-STAGE MEMBRANE REACTOR FOR OXIDATIVE COUPLING OF METHANE

Miss Sirikarn Tiraset

A Thesis Submitted in Partial Fulfillment of the Requirements
for the Degree of Master of Engineering Program in Chemical Engineering
Department of Chemical Engineering
Faculty of Engineering
Chulalongkorn University
Academic Year 2011

Thesis Title	THEORETICAL ANALYSIS OF A MULTI-STAGE MEMBRANE REACTOR FOR OXIDATIVE COUPLING OF METHANE
By	Miss Sirikarn Tiraset
Field of Study	Chemical Engineering
Thesis Advisor	Assistant Professor Amornchai Arpornwichanop, D.Eng.

Accepted by the Faculty of Engineering, Chulalongkorn University in Partial Fulfillment of the Requirements for the Master's Degree

……Dean of the Faculty of Engineering
(Associate Professor Boonsom Lerdhirunwong, Dr.Ing.)

THESIS COMMITTEE

……Chairman
(Assistant Professor Montree Wongsri, D.Sc.)

……Thesis Advisor
(Assistant Professor Amornchai Arpornwichanop, D.Eng.)

……Examiner
(Pimporn Ponpesh, Ph.D.)

……External Examiner
(Yaneeporn Patcharavorachot, D.Eng.)

สิริกาญจน์ ติรเศรษฐ์ : การวิเคราะห์ทางทฤษฎีของเครื่องปฏิกรณ์เมมเบรนแบบหลายขั้นสำหรับปฏิกิริยาคู่ควบของมีเทนแบบออกซิเดชัน. (THEORETICAL ANALYSIS OF A MULTI-STAGE MEMBRANE REACTOR FOR OXIDATIVE COUPLING OF METHANE) อ.ที่ปรึกษาวิทยานิพนธ์หลัก : ผศ.ดร.อมรชัย อาภรณ์วิชานพ, 88 หน้า.

ปฏิกิริยาคู่ควบของมีเทนแบบออกซิเดชันเป็นทางเลือกหนึ่งสำหรับการผลิตเอทิลีนจากก๊าซมีเทน อย่างไรก็ตามกระบวนการนี้จะให้ค่าการเลือกเกิดและผลได้ของเอทิลีนน้อยเมื่อเกิดการเปลี่ยนรูปมีเทนสูง เนื่องจากเกิดปฏิกิริยาออกซิเดชันของมีเทนและผลิตภัณฑ์ ซึ่งเป็นปฏิกิริยาข้างเคียงที่ไม่ต้องการ เพื่อแก้ไขข้อจำกัดดังกล่าว การประยุกต์ใช้เครื่องปฏิกรณ์แบบเมมเบรนโดยใช้เมมเบรนเป็นตัวกระจายออกซิเจนเพื่อป้องกันการเกิดปฏิกิริยาออกซิเดชันของผลิตภัณฑ์เอทิลีน จึงเป็นแนวทางหนึ่งที่น่าสนใจ ในงานวิจัยนี้ เครื่องปฏิกรณ์เมมเบรนแบบหลายขั้นถูกนำเสนอเพื่อเพิ่มสมรรถนะการเกิดปฏิกิริยาคู่ควบของมีเทนแบบออกซิเดชัน แบบจำลองทางคณิตศาสตร์ของเครื่องปฏิกรณ์แบบเมมเบรนที่ได้จากสมการอนุรักษ์มวลและพลังงาน และแบบจำลองทางจลนศาสตร์ของปฏิกิริยาถูกใช้ในการวิเคราะห์ผลของพารามิเตอร์ที่สำคัญ ได้แก่ อุณหภูมิ อัตราส่วนของมีเทนและออกซิเจนในสายป้อน และอัตราการไหลของมีเทน ที่มีต่อประสิทธิภาพของกระบวนการคู่ควบของมีเทนแบบออกซิเดชัน โดยพิจารณาจากค่าการเปลี่ยนมีเทน ค่าการเลือกเกิดผลิตภัณฑ์ และค่าผลได้ของผลิตภัณฑ์ นอกจากนี้ยังได้ศึกษาการปรับสัดส่วนของออกซิเจนในแต่ละขั้นของเครื่องปฏิกรณ์ภายใต้สภาวะอุณหภูมิคงที่และไม่คงที่ จากนั้นทำการเปรียบเทียบสมรรถนะของเครื่องปฏิกรณ์เมมเบรนแบบหลายขั้นกับเครื่องปฏิกรณ์เมมเบรนแบบขั้นเดียว ผลที่ได้พบว่า การนำเครื่องปฏิกรณ์เมมเบรนแบบหลายขั้นมาใช้กับปฏิกิริยาคู่ควบสามารถเพิ่มประสิทธิภาพของกระบวนการได้ นอกจากนี้งานวิจัยยังได้ใช้วิธีการออกแบบพื้นที่การตอบสนองเอพื่อหาสภาวะการดำเนินงานที่เหมาะสมของกระบวนการคู่ควบของมีเทนแบบออกซิเดชันเพื่อให้ได้ผลผลิตของเอทิลีนสูงที่สุด

ภาควิชา วิศวกรรมเคมี ลายมือชื่อนิสิต .....

สาขาวิชา วิศวกรรมเคมี ลายมือชื่อ อ.ที่ปรึกษาวิทยานิพนธ์หลัก .....

ปีการศึกษา 2554

537 06116 21 : MAJOR CHEMICAL ENGINEERING
KEYWORDS : OXIDATIVE COUPLING OF METHANE / MEMBRANE REACTOR / MULTI-STAGE REACTOR / FEED DISTRIBUTION / PERFORMANCE ANALYSIS

SIRIKARN TIRASET: THEORETICAL ANALYSIS OF A MULTI-STAGE MEMBRANE REACTOR FOR OXIDATIVE COUPLING OF METHANE.
ADVISOR: ASST. PROF. AMORNCHAI ARPORNWICHANOP, D.Eng., 88 pp.

Oxidative coupling of methane (OCM) is a promising route for the production of ethylene by fully utilizing the abundance of methane feedstock. However, this process suffers from the relatively low selectivity and yield of ethylene at a higher methane conversion due to the complete oxidation of methane and ethylene products. To overcome this limitation, the application of a membrane reactor in which oxygen selective membrane is used to prevent the deep oxidation of a desirable ethylene product is a potential alternative. In this study, a multi-stage dense tubular membrane reactor is proposed to improve the performance of the oxidative coupling of methane. Mathematic model of the membrane reactor based on conservative equations and detailed OCM kinetic model is employed to analyze the effect of key operating parameters such as temperature, methane-to-oxygen feed ratio and methane flow rate, on the efficiency of the OCM process in terms of CH_4 conversion, C_2 selectivity and C_2 yield. Adjustment of feed distributions at each membrane stage under isothermal and non-isothermal conditions is also studied. The performance of the multi-stage membrane reactor is compared with a single stage membrane reactor. The result shows that the distributed feeding policy improves the performance of the OCM process. A surface response technique is further employed to determine the optimal operating condition of the OCM process with the aim to maximize the C_2 products.

Department : Chemical Engineering Student's Signature .....
Field of Study : Chemical Engineering Advisor's Signature .....
Academic Year : 2011

ACKNOWLEDGEMENTS

First of all, I wish to express my greatest gratitude to my thesis advisor, Assistant Professor Amornchai Arpornwichanop, for his superior guidance on how to work independently as well as to indentify a problem and handle it with an optimal way. This led me to understand a wide variety of research and non-research areas. Apart from being a great mentor and colleague, he has also been a cornerstone for my professional development. My thesis would not be completed without his advices and professional comments.

I am deeply grateful to other member of my thesis committee, Assistant Professor Montree Wongsri, Dr. Pimporn Ponpesh and Dr. Yaneeporn Patcharavorachot, for their time and useful comments on this thesis.

Support from the Thailand Research Fund, Commission of Higher Education and the Computational Process Engineering research group, the Special Task Force for Activating Research (STAR), Chulalongkorn University Centenary Academic Development Project is also gratefully acknowledged.

I would like to thank all my friends who help me when I confront some difficulties. Thanks also to my colleagues in the Control and Systems Engineering Research Center for their friendship and support over the years of my study.

Last but not least, my greatest thankfulness goes to my family for their understanding and support. Without them, I would not be able to come this far. Thank you so much for being patience in waiting for me to complete my thesis.

CONTENTS

PAGE

ABSTRACT (THAI)..... iv
ABSTRACT (ENGLISH)..... v
ACKNOWLEDGEMENTS..... vi
CONTENTS..... vii
LIST OF TABLES..... xi
LIST OF FIGURES..... xii
LIST OF ABBREVIATIONS..... xv

CHAPTER

I INTRODUCTION..... 1
1.1 Introduction……..... 1
1.2 Objectives……..... 3
1.3 Scopes of research……..……..... 3
1.4 Expected benefits……..……..... 4

II LITERATURE REVIEWS……..... 5
2.1 Catalysts for oxidative coupling of methane….....……..... 5
2.2 Performance of OCM reactors.....……..……..... 7
2.2.1 A fixed bed reactor……..... 7
2.2.2 A membrane reactor..... 8
2.3 Kinetic study of OCM..... 10
2.4 Modeling and simulation of OCM..... 11
2.5 Optimization of OCM..... 12

III THEORY..... 15
3.1 Oxidative Coupling of Methane (OCM)..... 15

CHAPTER PAGE

3.1.1 Definition..... 15
3.1.2 Reaction scheme of OCM process..... 15
3.2 Membrane..... 16
3.2.1 Basic concepts of membrane separation processes..... 17
3.2.2 Membrane reactor concepts..... 20
3.3 Design of Experiment (DOE)..... 22
3.4 Response Surface Methodology (RSM)..... 23
3.5 Central Composite Design (CCD)..... 24
3.6 Analysis of variance..... 24

IV MATHEMATICAL MODEL OF MEMBRANE REACTOR FOR OXIDATIVE COUPLING OF METHANE..... 25
4.1 Membrane reactor..... 25
4.1.1 Single-stage membrane reactor..... 25
4.1.2 Multi-stage membrane reactor..... 26
4.2 Model equations..... 27
4.3 Kinetics of oxidative coupling of methane..... 29
4.4 Oxygen permeation rate of BSCFO tubular membrane..... 32
4.5 OCM performance..... 33
4.6 Model validation..... 33

V PERFORMANCE ANALYSIS OF MEMBRANE REACTOR FOR OXIDATIVE COUPLING OF METHANE..... 35
5.1 A single-stage membrane reactor..... 35
5.1.1 Concentration profiles..... 35
5.1.2 Effect of methane to oxygen feed ratio..... 37
5.1.3 Effect of operating temperatures..... 39
5.1.4 Effect of methane feed flow rate..... 41
5.1.5 Adiabatic operation..... 42
5.2 A multi-stage membrane reactor..... 44

CHAPTER PAGE

5.2.1 Oxygen concentration profile..... 44
5.2.2 Comparison of single- and multi-stage membrane reactors... 45
5.2.2.1 Effect of methane to oxygen feed ratio.....45
5.2.2.2 Effect of operating temperature..... 48
5.2.2.3 Effect of methane feed flow rate.....50
5.2.3 Effect of decreased oxygen feed with different proportions...52
5.2.4 Adiabatic operation.....53

VI OPTIMIZATION OF MEMBRANE REACTOR
FOR OXIDATIVE COUPLING OF METHANE.....55
6.1 Design of experiment.....55
6.2 Optimization of single-stage membrane reactor..... 58
6.2.1 Regression model equation for C_2 yield..... 58
6.2.2 Results.....60
6.2.2.1 Effect of one factor..... 61
6.2.2.2 Effect of an interaction between two variables.....61
6.2.3 Optimal operating parameters.....65
6.3 Optimization of multi-stage membrane reactor..... 66
6.3.1 Regression model equation for C_2 yield..... 66
6.3.2 Results.....70
6.3.2.1 Effect of one factor..... 70
6.3.2.2 Effect of an interaction between two variables.....70
6.3.3 Optimal operating parameters.....74

VII CONCLUSIONS AND RECOMMENDATION..... 76
7.1 Conclusions.....77
7.2 Recommendation..... 78

REFERENCES..... 79

PAGE

APPENDIX... 86

VITA... 88

LIST OF TABLES

TABLE PAGE

3.1 Types and properties of membranes..... 19
4.1 Heat capacity of gas species involved in the reactions..... 28
4.2 Kinetic parameters of the OCM reactions..... 31
4.3 Ambipolar diffusion coefficients (D_a) at different temperatures..... 32
4.4 Comparison between model prediction and experimental data (Stansch et al.,1997)..... 34
5.1 Operating conditions and reactor parameters..... 37
6.1 Experimental range and levels of independent process variables for OCM..... 55
6.2 Full factorial central composite design matrix of three independent variables in coded and unit along with the simulated response value..... 57
6.3 ANOVA of the response surface quadratic model for single-stage membrane reactor..... 60
6.4 Comparison between simulation result and model prediction of the single-stage membrane for OCM process operated at the optimum conditions..... 66
6.5 Full factorial central composite design matrix of three independent variables in coded and unit along with the simulated response value for a multi-stage membrane reactor (50-30-20)..... 68
6.6 ANOVA of the response surface quadratic model for multi-stage membrane reactor..... 69
6.7 Comparison between simulation result and model prediction of the multi-stage membrane for OCM process operated at the optimum conditions..... 75

LIST OF FIGURES

FIGURE PAGE

3.1 A general scheme of the reaction network in oxidative coupling of methane....16

3.2 Schematic diagrams of principal types of membranes....17

3.3 Basic membrane separation principle.... 18

3.4 Schematic diagram of various membrane reactor concepts for a tubular configuration (Mulder, 1996): (a) bore of the tube filled with catalyst; (b) top layer filled with catalyst; (c) membrane wall filled with catalyst....21

4.1 Membrane reactor.... 26

4.2 A multi-stage membrane reactor....26

5.1 Concentration profiles at the reaction side of the membrane reactor....36

5.2 Effect of CH_4/O_2 ratio on the conversion of methane and the selectivity and yield of C_2 product.... 38

5.3 Effect of CH_4/O_2 ratio on the C_2H_4/C_2H_6 product ratio....39

5.4 Effect of operating temperatures on the conversion of methane and the selectivity and yield of C_2 product....40

5.5 Effect of operating temperature on the C_2H_4/C_2H_6 product ratio.... 40

5.6 Effect of methane feed flow rate on the conversion of methane and the selectivity and yield of C_2 product....41

5.7 Effect of methane feed flow rate on the C_2H_4/C_2H_6 product ratio....42

5.8 Temperature profile along the reactor....43

5.9 Effect of inlet temperatures on the highest temperature and C_2 yield of the membrane reactor operated under non-isothermal condition.... 44

5.10 Concentration profile of oxygen at the tube side of membrane reactors.... 45

5.11 Effect of CH_4/O_2 ratio on single- and multi-stage membrane reactors....47

5.12 Effect of operating temperature on single- and multi-stage membrane reactors.... 50

FIGURE PAGE

5.13 Effect of methane feed flow rate on single- and multi-stage membrane reactors..... 52
5.14 C_2 yield of the multi-stage membrane reactor with decreased feed of oxygen.....53
5.15 Temperature profile along single- and multi-stage membrane reactor..... 54
5.16 Effect of inlet temperature on the C_2 yield of a multi-stage membrane reactor operated under isothermal and adiabatic conditions.....54
6.1 Predicted and actual values of C_2 yield for single-stage membrane reactor.....59
6.2 Effect of CH_4/O_2 ratio, temperature and CH_4 feed flow rate on C_2 yield in case of a single-stage membrane reactor..... 61
6.3 Contour surface plot of C_2 yield as a function of CH_4/O_2 ratio and operating temperature..... 62
6.4 3-D graphic surface optimization of C_2 yield versus CH_4/O_2 ratio and operating temperature.....62
6.5 Contour surface plot of C_2 yield as a function of CH_4/O_2 ratio and CH_4 feed flow rate.....63
6.6 3-D graphic surface optimization of C_2 yield versus CH_4/O_2 ratio and CH_4 feed flow rate..... 64
6.7 Contour surface plot of C_2 yield as a function of operating temperature and CH_4 feed flow rate.....64
6.8 3-D graphic surface optimization of C_2 yield versus operating temperature and CH_4 feed flow rate.....65
6.9 Predicted and actual values of C_2 yield for multi-stage membrane reactor..... 67
6.10 Effect of CH_4/O_2 ratio, temperature and CH_4 feed flow rate on C_2 yield in case of a multi-stage membrane reactor..... 70
6.11 Contour surface plot of C_2 yield as a function of CH_4/O_2 ratio and operating temperature..... 71

FIGURE PAGE

6.12 3-D graphic surface optimization of C_2 yield versus CH_4/O_2 ratio and operating temperature....71
6.13 Contour surface plot of C_2 yield as a function of CH_4/O_2 ratio and CH_4 feed flow rate....72
6.14 3-D graphic surface optimization of C_2 yield versus CH_4/O_2 ratio and CH_4 feed flow rate....73
6.15 Contour surface plot of C_2 yield as a function of operating temperature and CH_4 feed flow rate....73
6.16 3-D graphic surface optimization of C_2 yield versus operating temperature and CH_4 feed flow rate....74

LIST OF ABBREVIATIONS

A_{CS}	Cross section area of the tube side [cm^2]
C_i	Density of oxygen ions [mol cm^{-3}]
C_{p_i}	Heat capacity of specie *i* [J mol^{-1} K^{-1}]
D_a	Ambipolar diffusion coefficients [cm^2 s^{-1}]
d_1	Outer diameter of the membrane tube [cm]
d_2	Inner diameter of the membrane tube [cm]
$E_{a,j}$	Activation energy in reaction *j* [kJ mol^{-1}]
F_i	Molar flow rate of specie *i* [mol/s]
ΔH_i	Heat of reaction *i* [J mol^{-1}]
J_{O_2}	Oxygen flux through the membrane [mol cm^{-2} s^{-1}]
K_m	Average thermal conductivity [J s^{-1} m^{-1} K^{-1})
K_0	Kinetic parameter [mol $g^{-1}s^{-1}$ $Pa^{-(m+n)}$]
L	Length of the membrane tube [cm]
M	Membrane thickness [cm]
P_i	Partial pressure of component *i* [Pa]
q	Heat flux between the tube side and shell side [J m^{-1} s^{-1}]
r_j	Rate of reaction *j* [mol g^{-1} s^{-1}]
S	Effective area of the membrane tube [cm]
T	Temperature [°C]

V	Reactor volume [m^3]
W	Catalyst weight [g]

Greek Symbols

α	Star point for CCD
$\nu_{i,j}$	Stoichiometric coefficient of component *j* of reaction *i*

Superscript

t	Tube side
s	Shell side

CHAPTER I

INTRODUCTION

This chapter introduces the problem statement and importance of the study, objectives, scopes of research, expected benefit and research methodology.

1.1 Introduction

Ethylene is the most important base chemical in petrochemical industries for the production of polymers and ethylene derivatives such as ethylene oxide and ethylene glycol. Virtually, all ethylene worldwide is conventionally produced via a steam cracking of hydrocarbon feedstock ranging from light ethane/propane mixture to heavy naphtha and vacuum gas oils. As crude oil is limited and its demand is continuously increased, the price of feedstock for ethylene production increases as well. In the recent years, there is an increasing demand for ethylene all over the world; therefore, alternative technology with high potential to exploit available resource for ethylene production should be explored.

Methane is the main component of natural gas (NG) and biogas, and a by-product from oil refining and chemical industries. Conversion of methane to more useful chemicals and fuels is recognized as the next step to sustain economic growth and maintain fuel supplies (Lunsford, 2000; Bouwmeester, 2003). In addition, it could also reduce the severe greenhouse effect of CH_4 (Trevor et al., 1990). Different methodologies have been proposed to convert methane into olefins, higher hydrocarbons and gasoline via indirect and direct conversion processes. The indirect approach involve the production of synthesis gas (syngas), an intermediate, from methane and then transforms it into other chemicals via Fischer-Tropsch process, which causes a substantial energy loss. In contrast, the direct conversion process converts methane into higher hydrocarbons in one step. Among the various direct

process, the oxidative coupling of methane (OCM) is a promising technology to convert methane into ethylene and ethane.

Extensive studies on OCM processes have been conducted since the pioneer work of Keller and Bhasin in 1982. Many different reactor concepts, therefore, have been proposed for this process. Due to its technological simplicity, a fixed-bed reactor (FBR) is widely applied. The operation of this reactor is accident prone because of the large amount of heat released during the course of reaction. Furthermore, a poor heat removal from the highly exothermic reaction results in the occurrence of hot spots, affecting the reactor operation such as temperature runaway, catalyst deactivation, undesired side reactions and thermal decomposition of products (Follmer et al., 1988). Applying a fluidized-bed reactor, which has high heat transfer capacity, shows better heat management and temperature control than a fixed bed reactor system. Talebizadeh et al. (2009) studied the OCM over $Mn/Na_2WO_4/SiO_2$ catalyst in a two-zone fluidized-bed reactor (TZFBR) and its performance was compared with a fluidized-bed reactor. Although the TZFBR gave the C_2 selectivity larger than that in fluidized-bed reactor, the C_2 yield was still relatively low (< 20%).

The difficulty in the operation of OCM process lies in the fact that the intermediates and target products are higher reactive than the reactant and therefore are prone to deeply oxidize to CO_x. Thus, the oxidation of methane and C_{2+} products seems to be unavoidable when high oxygen content is present in the feed stream. The concept of using an oxygen distribution in a fixed-bed reactor was studied by Zarrinpashne et al. (2004) in order to improve the OCM performance. There are five oxygen feeding points along the reactor with precise control of oxygen flow rate at each point. However, the proposed reactor concept cannot achieve the high yield of ethylene due to the incomplete gas mixing at the oxygen feeding points. This causes high oxygen concentration zones at which the C_{2+} product is easily combusted and its selectivity falls significantly. Omata et al. (1989) initially applied a membrane reactor for the OCM process. The use of the membrane reactor to control oxygen concentration offers a possibility to achieve much higher C_2 hydrocarbons selectivity and yield. Mixed-conducting oxide membranes such as perovskite-type membranes, are well known for their abilities to separate oxygen from air. $Ba_{0.5}Sr_{0.5}Co_{0.8}Fe_{0.2}O_{3-\delta}$

(BSCFO), which was first reported by Shao et al. (2000), is a promising mixed conducting membrane with high oxygen permeability and has proven to be a good candidate for use as an oxygen distributor in the OCM reactor.

In this study, a dense tubular membrane reactor is investigated to improve the performance of the oxidative coupling of methane. A single stage and multi-stage membrane reactors are considered. A mathematic model of the membrane reactor based on conservative equations and detailed OCM kinetic model is employed to analyze the effect of key operating parameters such as temperature, methane to oxygen feed ratio and methane feed flow rate, on the efficiency of the OCM process in terms of CH_4 conversion, C_2 selectivity and C_2 yield. Adjustment of feed distributions at each membrane stage under isothermal and non-isothermal conditions is also studied. The performance of the multi-stage membrane reactor is compared with a single stage membrane reactor. The simulated data obtained are used for the optimization of the process conditions by the central composite design (CCD) of response surface methodology (RSM).

1.2 Objectives

The objectives of this study are to analyze the steady state performance of a single and multi-stage membrane reactor for an oxidative coupling of methane (OCM) and to determine the optimal operating condition of the OCM process with the aim to maximize the C_2 products.

1.3 Scopes of research

1.3.1 The research work is divided into three parts:

(i) To investigate the performance of a conventional single-stage membrane reactor for OCM process.

(ii) To investigate the performance of a multi-stage membrane reactor for OCM process.

(iii) To determine the optimum operating condition of the single-stage and multi-stage dense tubular membrane reactor by using a response surface methodology (RSM).

1.3.2 A mathematic model of a membrane reactor based on conservative equations, detailed OCM kinetic model proposed by Stansch et al. (1997) and the oxygen flux equation developed by Kim et al. (1998), is used and simulations are performed by using MATLAB.

1.3.3 The performance of membrane reactors in terms of CH_4 conversion, C_2 selectivity and C_2 yield is considered with respect to the effect of key operating parameters such as temperature, methane to oxygen feed ratio and methane feed flow rate.

1.4 Expected benefits

1.4.1 To improve the performance of OCM process by using a multi-stage membrane reactor.

1.4.2 To understand effects of key operating parameters on the performance of OCM process.

1.4.3 To determine optimum operating conditions for OCM process.

CHAPTER II

LITERATURE REVIEWS

The oxidative coupling of methane (OCM) was firstly studied by Keller and Bhasin (1982). Since then, a number of studies on the OCM process has been directed to the production of higher hydrocarbons, mainly ethylene. This process is considered a promising route for the conversion of natural gas to ethylene. OCM is classified as a direct methane conversion process without the formation of synthesis gas and has been the subject of interest because of its efficient energy usage. However, due to the complex reaction scheme, the implementation of OCM process to industrial scale is still limited. A number of researches on OCM process have been conducted intensively in order to improve its performance in terms of C_2 yield. A high yield of C_2 products (> 30%) is required for industrial applications. As a result, there are many studies concerned about the development of OCM catalyst, improvement of reactor performance, simulation and optimization of OCM process.

2.1 Catalysts for oxidative coupling of methane (OCM)

The most study in topic of OCM is catalyst synthesis and formulations in order to improving its performance. Several catalysts were investigated and found to be effective in this complex heterogeneous-homogeneous reactions. Many metal oxide catalysts have been tested for the OCM reaction. The catalysts can be grouped as: (i) oxides of groups 4 and 5 metals; (ii) oxides of group 3 metals; (iii) oxides of group 2 metals; (iv) oxides of group 1 metals; (v) lanthanide-based oxides; and (vi) transition metal oxides (Alvarez-Galvan et al., 2011). In the early studies, Li/MgO catalyst attracts attention of researchers in this field as a potential catalyst for OCM process since the first study of Driscoll in 1985. Ito et al. (1985) also studied of Li/MgO for OCM and began a fundamental study on methyl radical formation resulted in the discovery of a new class of catalyst for the conversion of CH_4 to higher hydrocarbons

in the presence of oxygen. Choudhary et al. (1998) used La_2O_3 and alkaline earth promoted La_2O_3 catalysts and the results showed that those are good catalysts for OCM as well.

Other catalysts that had extensive studies done by many researchers on OCM process were Na-W-Mn-based catalysts (Pak et al., 1998; Ji et al., 2002; Chua et al., 2008). Ji et al. (2002) used Na-W-Mn/SiO_2 as the catalyst and found that it shows good activity for OCM process. The catalyst combines SiO_2 with tungsten (W) and manganese (Mn) from transition metals group and impregnates it with sodium (Na). The addition of Na increases the concentration of surface active oxygen by improving the migration of Mn to the catalyst surface, as both elements are found in high concentration in this area. The CH_4 conversion and C_2 selectivity are closely related to the surface Mn concentration of the catalysts. Both Na-O-Mn and Na-O-W act as the active centers of the catalysts for OCM. There is a synergic effect of Na, W, and Mn components, and the $Na_2W_2O_7$ crystalline phase is found to be active in OCM reaction.

Huang et al. (2003) designed a six components Na-W-Mn-Zr-S-P/SiO_2 catalyst. They applied a combination of genetic algorithm (GA) and artificial neural networks (ANN) using six metal components for catalyst synthesis. Following this, a sample was found, which was able to give 27.8% yield of C_{2+} products per pass. Compared to Na-W-Mn/SiO_2 catalyst, the six-component catalyst showed higher activity at a low temperature in the OCM reaction without any dilute gas. Subsequently, they investigated the effect of S and P promoters on the performance of the Na-W-Mn-Zr/SiO_2 catalyst, and concluded that the addition of S and P improved the catalytic activity by increasing the concentration of lattice oxygen in metal oxides (MO_x).

Zheng et al. (2010) also studied of six-component Na-W-Mn-Zr-S-P/SiO_2 catalysts prepared by different methods for oxidative coupling of methane. The catalysts were prepared by incipient wetness impregnation, sol-gel and mixture slurry methods. Among all the catalyst samples tested, the catalyst prepared by mixture slurry method showed the highest catalytic activity for OCM. Furthermore, the effects

of different addition sequences of each component on the performance of catalyst were studied. The results showed that the absence of Na before the addition of Mn and Zr in the catalysts preparation method decreased the formation of the active phases of Mn_2O_3 and ZrO_2 and also decreased the activities of the catalysts significantly.

2.2 Performance of OCM reactors

Many different reactor configurations and concepts were proposed to be studied for the oxidative coupling of methane, such as fixed bed reactor, fluidized bed reactor, solid oxide fuel cell reactor, catalytic dense membrane reactor, porous membrane reactor. All of those reactor concepts are having their advantages and drawbacks. There have been extensive research and development efforts in designed reactors in order to obtaining a high yield and selectivity in the OCM process.

2.2.1 A fixed bed reactor

Fixed bed reactor represents a state of the art in the industry, and has to be examined in detail (Jašo et al., 2010). So far, the fixed-bed reactor has been widely used for OCM due to its technological simplicity and easy operation. Ji et al. (2002) used Na-W-Mn/SiO_2 catalyst while Hong et al. (2001) carried out OCM with $CaCl_2$-promoted calcium chlorophosphate catalysts in a micro-test fixed bed reactor and obtained promising results. Zeng (2001) also used a fixed bed reactor but operated it in a co-feed mode using dense fluorite-structured $Bi_{1.5}Y_{0.3}Sm_{0.2}O_{3-\delta}$ (BYS) pellets achieved C_2 yield of 26% with C_2 selectivity up to 60%. Many studies on this reactor type were done, and the major barrier is severe hot spots, incurred as a result of poor heat removal from the highly exothermic reactions. The hot spots are not only weakens the catalytic performance, but also may lead to an explosion under the temperature runaway condition.

Liu et al. (2008) presented scale up and stability test for oxidative coupling of methane over Na_2WO_4-Mn/SiO_2 catalyst in a 200 ml fixed-bed reactor. The effects of

operating parameter in terms of temperature, CH_4/O_2 molar ratio, steam (diluent), and methane GHSV were studied. The results indicated that the gas-phase reaction was increased and a large amount of methane was converted into CO_x with increasing reaction temperature. The higher selectivity and yield of C_2 products were obtained under suitable operating conditions, such as, high CH_4/O_2 ratio, low GHSV, and the presence of a large amount of steam, which decreased the released heat energy or transferred it quickly from the catalyst bed. The C_2 selectivity of 61%−66% and C_2 yield of 24.2%−25.4% were achieved by a single pass without any significant loss in catalytic performance in reaction time of 100 hours.

2.2.2 A membrane reactor

The difficulty in OCM process lies in the fact that intermediates and target products are usually more reactive than the raw materials. So, if there is too much oxygen, it will lead to more oxidation reaction than the coupling reaction. To achieve an economically attractive C_2 yield (> 30–40%), considerable interests have been expressed in recent years in the development of various membrane reactors. By the addition of oxygen discretely through a membrane along the length of the reactor or membrane acts as oxygen distributor. The application of membrane reactors to control oxygen concentration along the reactors is a possibility to achieve much higher C_2 products selectivity and yield for OCM.

Kao et al.(2003) presented a simulation study of the oxidative coupling of methane in porous membrane reactor (PMR) packed with Li/MgO catalyst by the fixed-bed reactor (FBR) model with reliable reaction kinetic equations. PMR can enhanced the production of ethylene by controlling the amount of oxygen feed to the catalyst bed via handling its feed pressure. It was found that, at a fixed methane feed rate, there was an optimal oxygen feed pressure that would be achieve the highest yield of ethylene. With a commercial ultrafiltration membrane, theoretical analysis showed that PMR at the same dimension used in the FBR can achieved 30% yield at 53% selectivity. The results showed that the lower membrane permeability can

improved the OCM performance. Higher oxygen feed pressure reduced the yield as well as the selectivity.

Wang et al.(2005) studied the oxidative coupling of methane (OCM) in a dense membrane tube made of $Ba_{0.5}Sr_{0.5}Co_{0.8}Fe_{0.2}O_{3-\delta}$ (BSCFO). When the membrane tube was used as a catalytic membrane reactor for the OCM reaction without an additional catalyst, the C_2 selectivity had 20% increase compared to the packed-bed reactor using BSCFO as catalyst. A higher oxygen concentration in the product stream decreased the C_2 selectivity. The C_2 selectivity limitation may be due to the higher oxygen ion recombination rate, which was not only competed with the surface methane activation, but also led to the formation of gaseous oxygen and subsequent C_2 combustion. If an active OCM catalyst (La-Sr/CaO) was packed in the membrane tube, both C_2 selectivity and CH_4 conversion were improved compared to the blank run. The C_2H_4/C_2H_6 ratio in the membrane reactor with the La-Sr/CaO catalyst was much higher than that in the packed-bed reactor.

Bhatia et al.(2009) studied the oxidative coupling of methane in a catalytic membrane reactor (CMR), catalyst packed bed reactor (PBR) and catalyst packed bed membrane reactor (PBMR) respectively. The CMR consists of a mixed ionic-electronic conducting membrane (MIECM) with $Ba_{0.5}Ce_{0.4}Gd_{0.1}Co_{0.8}Fe_{0.2}O_{3-\delta}$ (BCGCF) material coating on the outer surface of ceramic tubular support using sol–gel method. A 3-components catalyst Na-W-Mn was coated as a catalytic thin film on the alumina tube using mixture slurry dip coating method. The CMR was designed and fabricated by considering the three major prerequisites such as, gas-tight reactor system, resistant to high temperature without any reaction with the gases and the membrane tube within the reactor could be taken out easily without damaging the membrane tube. A comparative performance study of PBR, PBMR and CMR reactor showed that the catalyst in PBR gave highest C_{2+} selectivity. The CMR performed best among three reactors with C_{2+} yield of 34.7% with methane conversion of 51.6% and C_{2+} selectivity of 67.4%. The PBMR did not perform well compared to PBR and CMR due to the leakage of gas.

Olivier et al.(2009) presented a comparative study of modifying an ionic oxygen conducting membrane reactor for the oxidative coupling of methane with 3 different catalytic surface modifications. Dense $Ba_{0.5}Sr_{0.5}Co_{0.8}Fe_{0.2}O_{3-\delta}$ (BSCFO) membrane disks were wash-coated with a MgO model catalyst and Pt was added by impregnation, using tetraammine platinum(II) nitrate as metal precursor (Sigma-Aldrich). The role of the catalyst was underlined by the fact that the LaSr/CaO gave the highest yield between 900 and 1000 °C while yields decline for the Sr/La_2O_3 catalyst at temperatures above 900 °C. It was obvious that a suitable catalytic modification of the membrane surface was essential for obtaining an attractive performance. The wash-coated Pt/MgO model catalyst suffered essentially from its low activity and had a smaller extent from the fact that the ethane to ethylene ratio remained comparably high. Both oxide based catalysts, Sr/La_2O_3 and LaSr/CaO, allowed to attain better activities, but the slightly high conversions and higher selectivity were observed.

2.3 Kinetic study of OCM

Kinetics of oxidative coupling of methane reaction to C_2 hydrocarbon products has been studied extensively based on the various reaction mechanisms. Indeed, kinetics of OCM reaction is very complicated in terms of proposed mechanism since it involves several chemical species (Su et al., 2003; Couwenberg et al., 1996; Xin et al., 2008). Sadeghzadeh Ahari et al. (2009) studied the application of a simple kinetic model for the oxidative coupling of methane to the design of effective catalysts. Firstly, they reviewed past research on the kinetics with regard to the above criteria, and determine a method to apply to the design of practical OCM catalysts. The review was given the following classification: (A) spectroscopic studies of O^- species and the reaction with methane, (B) kinetic simulation of gas phase reactions, (C) kinetic simulation of both gas phase and surface reactions, (D) kinetics integrating many radical reactions of single or several reactions, (E) surface kinetics focusing on methane consumption, and (F) power rate law expression of C_2 (ethane and ethylene) and C_1 (CO and CO_2) formation. Farsi et al. (2010) studied the kinetics of OCM reaction and classifies them as the same as Sadeghzadeh Ahari et al. (2009).

Daneshpayeh et al. (2009) modeled kinetics of oxidative coupling of methane over $Mn/Na_2WO_4/SiO_2$ catalyst, using experimental data of a micro catalytic fixed bed reactor and the genetic algorithm as parameter estimation method. In order to choose the best OCM reaction network for developing a comprehensive kinetic model over this catalyst, they compared five OCM reaction networks such as Stansch et al. (1997) over La_2O_3/CaO, Sohrabi et al. (1996) over $CaTiO_3$, Lacombe et al. (1995) over La_2O_3, Olsbye et al. (1992) over $BaCO_3/La_2O_n(CO_3)_{3-n}$ ($n > 1.5$), and Traykova et al. (1998) over La_2O_3/MgO. They found that almost all reaction steps considered in the models, reaction network for the OCM proposed by Stansch et al. has the best precision in comparison with the other models.

Sun et al. (2008) developed a detailed microkinetic model for oxidative coupling of methane. The reaction network contains 39 elementary steps among 13 molecules and 10 radicals and describes the gas-phase reactions and 14 catalytic reactions. The microkinetic model included the set of catalyst descriptors of Li/MgO and Sn/Li/MgO, which had been used as an example to illustrate the model performance. The simulations of two catalysts of OCM indicated that catalyst descriptor provided the capability to capture the chemical information from experiments of different catalysts. The microkinetic model including catalyst descriptors was able to describe the large amount of data of different catalysts produced by high-throughput technology.

2.4 Modeling and simulation of OCM

Ching et al. (2002) developed a one-dimensional model for the oxidative coupling of methane over La_2O_3/CaO catalyst in a fixed bed reactor. The system was assumed to be under steady state. The validity of the model was verified by comparing the model predictions of differential kinetics with experimental results for OCM that reported by Stansch et al. (1997). The model was used to simulate OCM reaction under three operational modes including isothermal, adiabatic and non-isothermal condition. A set of 10-step kinetic model of OCM that reported by Stansch was used in this process simulation. The parameters studied were methane to oxygen

(CH_4/O_2) ratio, temperature, space velocity, dilution effect of N_2 and H_2O in the feed. High CH_4/O_2 ratio favored the OCM reaction but it gave low yield of ethylene due to inadequate oxygen dose under isothermal mode. CH_4 conversion, selectivity and yield of C_2 increased with increasing temperature and a maximum value of yield was obtained at 1098 K. Nouralishahi et al. (2007) also used this model in their research to determine an optimal temperature profile in an OCM plug flow reactor for the maximizing of ethylene production. The problem was solved by using a defined performance index and the optimal temperature profile was found by using piecewise linear continuous optimal control by iterative dynamic programming. The results showed that the quantity of ethylene production by applying the optimal temperature profile is about 42% greater than that of the best performance of the reactor at 1096.3 K under isothermal condition. The higher amount of oxygen used at the entrance of the reactor would vanish later which in turn leads to a delayed rise of temperature.

Prodip et al. (2009) studied of modeling and simulation of simulated countercurrent moving bed chromatographic reactor (SCMBR) for oxidative coupling of methane. They created a mathematical model of the five SCMCR for OCM, which is peculiarly important for understanding the operation of this SCMCR system. A simple mathematical model that mimic the experimental conditions was developed and solved by using numerically tuned kinetic and adsorption parameters. The effects of the different operating variables such as switching time, flow rate in section P, feed flow rate, raffinate flow rate, eluent flow rate, and methane to oxygen make-up fed ratio on the concentration profiles of the five components were investigated as well as the conversion of CH_4; selectivity and yield of C_2H_6 and C_2H_4 were explained with respect to the trend for each of the single effect.

Jaˇso et al. (2010) studied the attainable performance of the OCM process in diverse configurations of a fixed-bed reactor, and two different feeding structures of packed bed membrane reactors using different catalysts such as La_2O_3/CaO, $Mn/Na_2WO_4/SiO_2$, and PbO/Al_2O_3, in a wide range of operating conditions. The effect of several variables such as operating temperature, membrane thickness, methane-to-oxygen ratio, feed flow rate, gas streams composition, and reactor length were investigated. Each of the proposed reactor structures showed relevant

performance aspects concerning the OCM process (e.g. selectivity or conversion) and its specific feeding policy. For instance, obtaining a high CH_4 conversion in the FBR structure or earning a high products selectivity in the CPBMR structure, where oxygen was supplied in a more controllable way, were the potential of these structures, respectively.

2.5 Optimization of OCM

Istadi and Amin (2006) determined the optimal process parameters and catalyst compositions of CO_2 oxidative coupling of methane (CO_2-OCM) process over CaO–MnO/CeO_2 catalyst using response surface methodology (RSM). A central composite rotatable design (CCRD) for four factors , i.e. CO_2/CH_4 ratio, reactor temperature, wt.% CaO and wt.% MnO in the catalyst, was employed for experimental design in which the variance of the predicted responses, i.e. CH_4 conversion, C_2 hydrocarbons selectivity and yield. The RSM approach for the empirical modeling of CO_2-OCM process had several advantages: (a) the response values at certain ranges of process parameters and catalyst compositions can be accurately predicted by the models, (b) the optimal value of each response can be obtained at the corresponding optimal process parameters and catalyst compositions, (c) the operating conditions and catalyst compositions suitable for the CO_2-OCM process can be recommended. With the multi-responses optimization, the search for the simultaneous optimal values of the C_2 selectivity and yield was performed using weighted sum of squared objective functions (WSSOF) technique. The results indicated that both individual and multi-responses optimization were useful for the suggestion of optimal process parameters and catalyst compositions for the CO_2-OCM process.

Amin and Pheng (2006) also used central composite experimental design and response surface methodology to determine the best operating conditions for maximizing the ethylene production. The operating temperature, inlet O_2 concentration and F/W were the three parameters pertaining to operating conditions. The coefficients of second-order polynomial equation models were established by

using the method of least squares. These models were used to estimate the values of responses in terms of C_2H_4 yield, C_2H_4 selectivity and CH_4 conversion based on the experimental data. The analysis of variance (ANOVA) was used for checking the significance of the second-order models and the results showed that these models gave good estimation of the process responses.

CHAPTER III

THEORY

3.1 Oxidative Coupling of Methane (OCM)

3.1.1 Definition

The oxidative coupling of methane (OCM) involves the reaction of CH_4 and O_2 over a catalyst at high temperatures (around 800°C) to form ethane (C_2H_6) and ethylene (C_2H_4). It is a single-step conversion of methane and highly exothermic reaction. This process converts methane into C_2 hydrocarbons by coupling two methyl radicals after the abstraction of a hydrogen atom from each methane molecule. However, the selectivity of C_2 products is always reduced due to the formation of undesired gases directly from the combustion of methane, intermediates and C_2 products. In the OCM process, the following main reactions and side reaction reactions occur simultaneously:

Main reaction :

$$2CH_4 + 1/2O_2 \rightarrow C_2H_6 + H_2O \quad (3.1)$$

$$C_2H_6 + 1/2O_2 \rightarrow C_2H_4 + H_2O \quad (3.2)$$

Side reaction :

$$CH_4 + 3/2O_2 \rightarrow CO + 2H_2O \quad (3.3)$$

$$CH_4 + 2O_2 \rightarrow CO_2 + 2H_2O \quad (3.4)$$

$$C_2H_6 + 7/2O_2 \rightarrow 2CO_2 + 3H_2O \quad (3.5)$$

3.1.2 Reaction scheme of OCM process

The reaction mechanism of OCM is very complex due to the reactions between reactants in gas phase reactions and heterogeneous reactions over bulk and surface catalyst, respectively. A general scheme of the reactions involving reactants

and products is shown in Figure 3.1. Oxygen is required to activate the catalyst and interacts strongly with the surface by dissociative reversible adsorption (Lin et al., 1987). The catalyst used in OCM not only produces radicals but also acts as an important radical quencher. There are two types of surface oxygen, active (such as oxygen anion radicals or adsorbed oxygen) and less active oxygen (such as lattice oxygen). A small number of active oxygen species react with methane to form methyl radical after the abstraction of a hydrogen atom from each methane molecule and then formation of ethylene by coupling two methyl radicals. Moreover, methyl radicals and C_2 products are prone to deeply oxidize to CO_x gas.

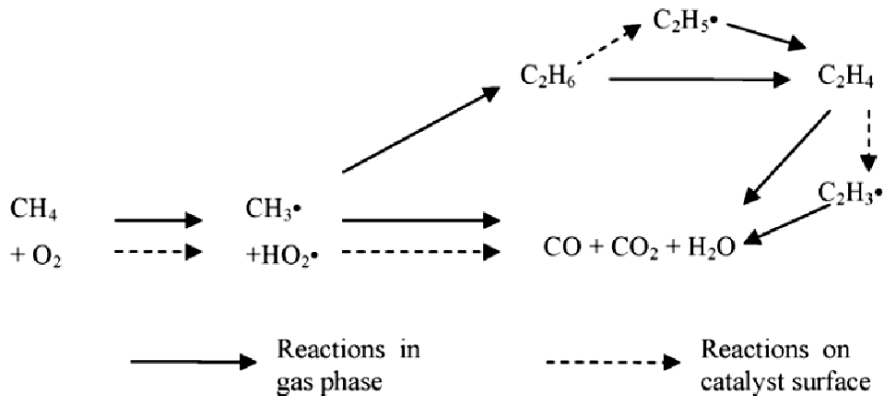

Figure 3.1 A general scheme of the reaction network in oxidative coupling of methane.

3.2 Membrane

The membrane is a selective barrier that separates two phases and restricts transport of various chemicals. Generally, it can be even classified into homogeneous or heterogeneous, symmetric or asymmetric in structure, solid or liquid; it can possess a positive or negative charge as well as it can be neutral or bipolar. The transport of matter from one point to another may be caused by convection or by diffusion of individual molecules, induced by an electric field or concentration, pressure or temperature gradient. The membrane thickness may vary from as small as 10 microns to few hundred micrometers. The principal types of membrane are shown schematically in Figure 3.2 and can be classified as below**:**

- Isotropic membranes
  - Microporous membranes
  - Nonporous, dense membranes
  - Electrically charged membranes
- Anisotropic membranes
- Ceramic, metal and liquid membranes

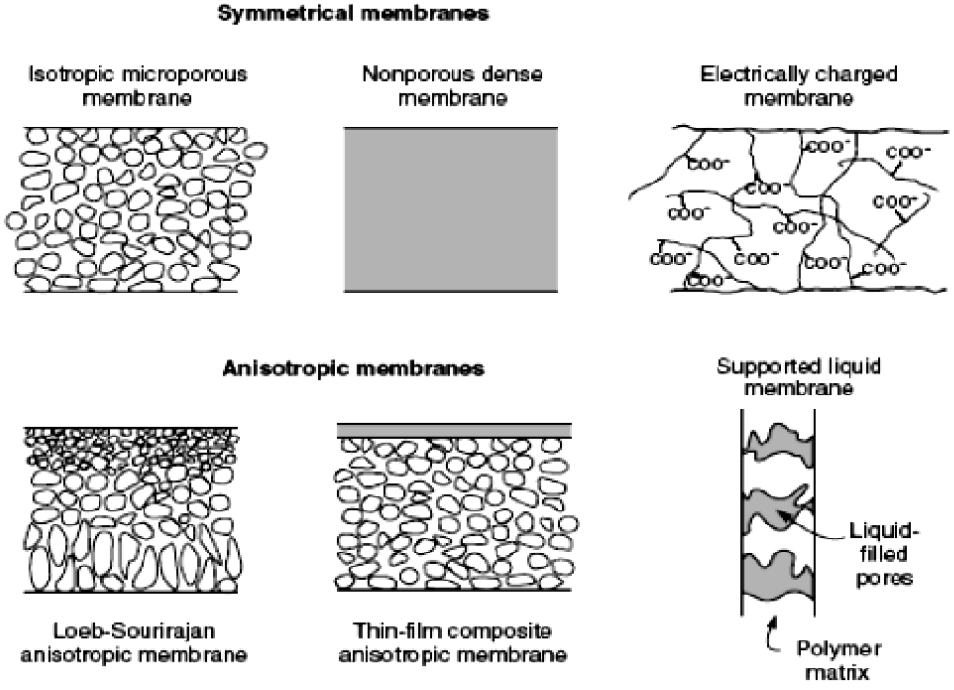

Figure 3.2 Schematic diagrams of principal types of membranes (Baker, 2004).

3.2.1 Basic concepts of membrane separation processes

The concept of membrane-based separation has been found at the early 18th century and believed that it is more useful than most of the traditional separation processes (distillation, adsorption, absorption, etc.) in energy savings and reduction in the initial capital investment requirements (Hsieh, 1996). Membranes are usually shaped as a thin film with permeable or semi-permeable or selective phase that acts as a barrier or container wall for the separation of chemical substances. The basic membrane separation process is illustrated in Figure 3.3; where the stream rejected by

a membrane is called retentate, while that passing through the membrane is called as permeate. Two of the most important characteristic property that describe the separation performance of a membrane are its permselectivity and permeability. Permeability denotes the flux of mass through a membrane per unit of area; whereas the permselectivity is the ability of the membrane to separate the permeate from the retentate.

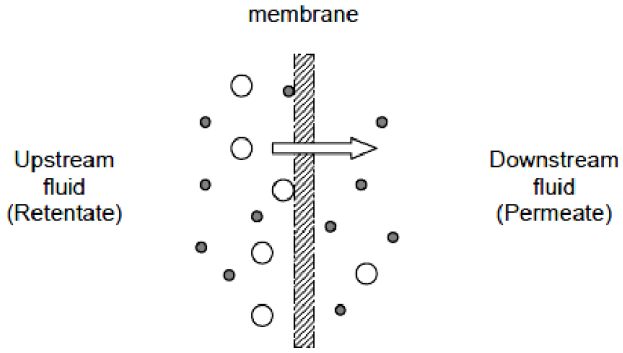

Figure 3.3 Basic membrane separation principle.

In the separation process, the structure and transport properties of commercial membranes are determined by the nature of them, in which the driving force (e.g. pressure gradient, concentration gradient, electrical potential, temperature, etc.) across the membrane is highly dependent to the type of membrane. The classification of membrane type and its characteristic involved the particular transport processes were classified as in Table 3.1.

Table 3.1 Types and properties of membranes (Baker, 2004)

Type of membrane	**Description**
Isotropic membranes (Symmetric membranes) Macroporous membranes	- Average pore diameters larger than 50nm - Molecular, Knudsen diffusion and convective flow as the transport mechanisms
Mesoporous membranes	- Average pore diameters in the intermediate range between 2 and 50 nm - Molecular, Knudsen diffusion and convective flow as the transport mechanisms
Microporous membranes	- Pore diameters smaller than 2 nm - Separation of solutes in molecular, pore-flow and Knudsen diffusion depending upon the solutes in the fluid mixture
Nonporous, Dense membranes	- Transport of solutes by driving force of a pressure, concentration or electrical potential gradient - Separation of components in a mixture is determined by their diffusivity and solubility in the membrane material
Electrically charged membranes	- Consist of pore walls carrying charged ions - Separation is determined by exclusion of ions of the same charge as the fixed ions of the membrane structure, rather than by the pore size
Anisotropic membrane (Asymmetric membrane)	- Consists of an extremely thin surface layer supported on a much thicker, porous substructure - Separation properties and permeation rates based on the surface layer.

The inorganic membrane has higher thermal and chemical resistance as well as a longer lifetime than the polymer membrane, but the structural change due to sintering and/or phase transformation occurred at elevated temperature that might alter the micro porous structures of inorganic membranes.

3.2.2 Membrane reactor concepts

The concept of combining the two unit operations, membrane and reactor, is being explored in various configurations, which can be classified in three groups, regarding the role of the membrane in the process. The membrane can be used to serve multiple functions. There are an extractor (the removal of product increases the conversion by shifting the reaction equilibrium), a distributor (the controlled addition of reactant along the reactor wall limits side reactions), or an active contactor (the controlled diffusion of reactants to the catalyst can lead to an engineered catalytic reaction zone). The distributor mode of membrane is normally well applied to restrict the parallel deep oxidation reactions of products for partial oxidation of hydrocarbons, oxidative dehydrogenation of hydrocarbons and oxidative coupling of methane.

Several catalytic processes of industrial necessary, however, often involve in harsh chemical environments and under high operating temperature, two factors that strongly favors inorganic membranes. Thus, glass, ceramic and metal membrane materials have been a dramatic surge of interest in the field of membrane reactor or membrane catalysis. Some promising applications using inorganic membranes include certain dehydrogenation, hydrogenation and oxidation reactions such as formation of butadiene from butane by dehydrogenation, styrene production from dehydrogenation of ethyl benzene, dehydrogenation of ethane to ethylene, water-gas shift reaction and oxidative coupling of methane, to name just a few (Hsieh, 1996).

The catalyst must be combined with the membrane system and various arrangements are possible. Figure 3.4 summarizes some membrane-catalyst combinations for tubular membranes (Mulder, 1996).

The most simple and straightforward system is where the catalyst is located inside the bore of the tube (Figure 3.4a). The advantage of this system is its simplicity in preparation and operation and in case of catalyst poisoning a new catalyst can easily be introduced. In the other two arrangements the catalyst is immobilized onto the membrane, either in the top layer (Figure 3.4b) or in the membrane wall (Figure 3.4c). In either case one of the products, not necessarily the required product, should permeate across the membrane which implies the necessity of permselective membranes under these specific conditions. At certain concentrations or partial pressures and at a certain temperature and pressure the equilibrium is completely fixed and thermodynamically determined. However, by removing one of the end products the reaction is shifted to the right hand side and results in an enhanced conversion rate.

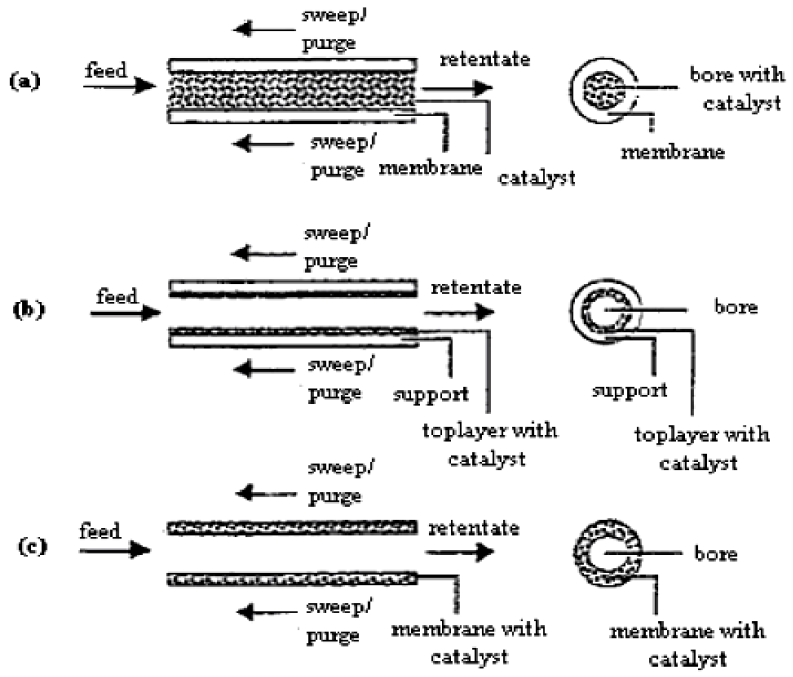

Figure 3.4 Schematic drawing of various membrane reactor concepts for a tubular configuration (Mulder, 1996): (a) bore of the tube filled with catalyst; (b) top layer filled with catalyst; (c) membrane wall filled with catalyst.

3.3 Design of Experiment (DOE)

In most of research and individual settings, the results are obtained from experimental methods for any different purposes. The main targeted of scientific research and process production are usually to show the statistical significance of the effect that a particular factor exerts on the dependent variable of interest (e.g., yield of products) and specify the optimum settings for different factors that affect the production process. In research and industrial settings, the primary goal is usually to extract the maximum amount of information regarding the factors affecting a production process from as few observations as possible. While in the former application analysis of variance (ANOVA) techniques are used to uncover the interactive nature of reality, as manifested in higher-order interactions of factors, in Indus "nuisance" (Cornell, 1990).

In general, every machine used in a production process allows its operators to adjust various settings, affecting the resultant quality of the product manufactured by the machine. Experimentation allows the production engineer to adjust the settings of the machine in a systematic manner and to learn which factors have the greatest impact on the resultant quality. Using this information, the settings can be constantly improved until optimum quality is obtained. Therefore, when DOE is applied in this study, combination of all factors involved with certain values will produce optimum response.

Experimental methods are finding increasing use in manufacturing to optimize the production process. Specifically, the goal of these methods is to identify the optimum settings for the different factors that affect the production process. In the discussion so far, the major classes of designs that are typically used in industrial experimentation have been introduced: 2**(k-p) (two-level, multi-factor) designs, screening designs for large numbers of factors, 3**(k-p) (three-level, multi-factor) designs (mixed designs with 2 and 3 level factors are also supported), central composite (or response surface) designs, Latin square designs, Taguchi robust design analysis, mixture designs, and special procedures for constructing experiments in constrained experimental regions. Interestingly, many of these experimental

techniques have "made their way" from the production plant into management, and successful implementations have been reported in profit planning in business, cash-flow optimization in banking (statsoft, 1999).

3.4 Response Surface Methodology (RSM)

Response surface methodology (RSM) is a set of technique design to find the best value of response. It discovers the best value or values of the response beyond the available resources of the experiments. This technique consists of designing the experiment and the subsequent analysis of the experiment data. In most cases, the behavior of the measured response is governed by certain laws that can be approximated by a deterministic relationship between the response and the set of experimental factors, and thus it is possible to determine the best condition (level) of factor to optimize a desired output.

The RSM is initiated with DOE to screen model-parameters before going to the optimization process (Montgomery, 1995). The DOE can effectively select the parameters of importance and indicate their interactions that significantly affect the response variables. Therefore, via DOE, RSM easily optimize the values of model parameters that are used in the model to produce the best fit between simulated and observed responses. The benefits of RSM are that it can determine the effects of parameter interactions on the response, it has a high ability to guide researchers to select the best model of response surface to adjust the best values of parameters, it is more systematic and accurate in guiding researcher to find the optimum, and finally the design and analysis can be conducted using standard statistical software without the need to write custom programs for a particular model.

The first step in experimental strategy of RSM is to decide on a model from which the response as a function of the independent variables in the process. This model provides the basis for new experimentation, which in turn may lead to a new model, and the entire cycle is repeated. The experimentation can be terminated at any time and further experimentation appears uneconomical. Finally, the sequential fitting of the model is prelude to the determination of optimum operating condition for a

process. By applying a mathematical equation or polynomial model the relationship between the true values and the quantitative factors can be represented by the graph contour plot.

3.5 Central Composite Design (CCD)

Central composite design (CCD) is very popular among researchers to analyze the influence of variables. CCD allowed us to show which variables significantly affect each response and optimize the value of variables that were found significant (Monteagudo et al., 1992).

The design is created from either factorial or fractional factorial design. For instance, CCD with three experimental factors employed 16 experiments. This experiment containing eight run at two level (-1/+1), six star point (-α/α) and two replicates at the center points (0) to allow estimation of the error and provide a check on linearity.

3.6 Analysis of Variance

To analyze the result more critically, a more efficient method to use is analysis of variance (ANOVA), which examines all sample and means them together. Basically, it is a simple arithmetical method of sorting out the components of variation in a given set of data and providing test of significance. The two principles involved are partition of sums of the squares and estimating the variance of population by different methods and comparing these estimates. The result of the analysis of a set experiment data and modeling can be displayed in table known as the ANOVA. The table will show the relationship between the observed data and predicted data and the calculation on sum of square that gives the result for analysis of variance.

CHAPTER IV

MATHEMATICAL MODEL OF MEMBRANE REACTOR FOR OXIDATIVE COUPLING OF METHANE

This chapter presents a mathematical model of oxidative coupling of methane (OCM) in membrane reactor. This model is used to simulate the OCM process by MATLAB software and investigate its performance. The first Section 4.1 shows the configuration of membrane reactor system used in this study. Section 4.2 describes the details of model equations. Kinetic equations of OCM and the oxygen permeation flux equation are described in Section 4.3 and Section 4.4. Section 4.5 illustrates the equations used to evaluate the performance of OCM process. Further, the validation of kinetic model used in this study is demonstrated in Section 4.6.

4.1 Model configuration

The membrane reactors considered in this study are a single stage dense tubular membrane reactor and a multi-stage one. A design of multi-stage membrane reactor is investigated to improve the process performance.

4.1.1 Single-stage membrane reactor

The configuration of a tubular membrane reactor for OCM considered in this study is schematically represented in Figure 4.1. The membrane reactor considered consist of two concentric tubes: the outer tube is the shell; the inner tube is the dense $Ba_{0.5}Sr_{0.5}Co_{0.8}Fe_{0.2}O_{3-\delta}$ membrane. The methane is fed into the tube side of the reactor, while the oxygen is fed into the shell side. The oxygen in the shell side permeates into the tube side through the membrane, which acts as an oxygen

distributor, and reacts with methane. The La_2O_3/CaO catalyst is packed in the tube side and, as a result, only the gases at the tube side are in direct contact with it and participated in the reaction.

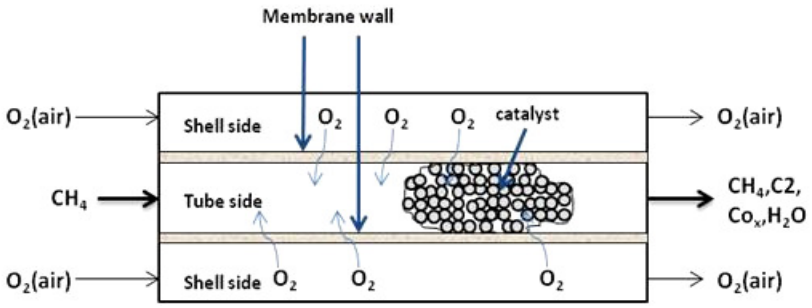

Figure 4.1 Membrane reactor

4.1.2 Multi-stage membrane reactor

The schematic diagram of a multi-stage membrane reactor is shown in Figure 4.2. Three arrangements of oxygen feeding distribution are considered: (i) increased feed (e.g. 10-30-60 (mol%)), (ii) uniform feed (e.g. 33-33-33 (mol%)) and (iii) decreased feed (e.g. 60-30-10 (mol%)). The La_2O_3/CaO catalyst is packed in every stage of membrane reactors. The length of a series connection membrane reactor is equal to a single tubular membrane reactor. The total amount of oxygen feeding and catalyst in each stage of a multi-stage membrane reactor are equal to that in a single stage one as well.

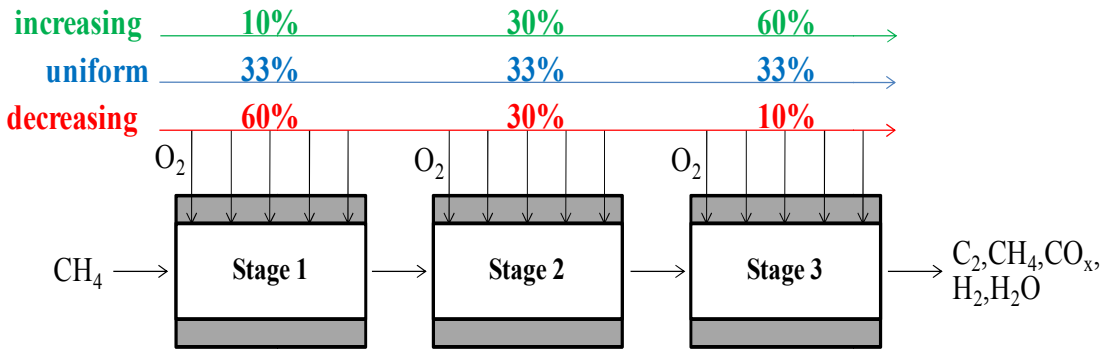

Figure 4.2 A multi-stage membrane reactor

4.2 Model equations

The mathematical model of the membrane reactor is based on the following assumptions:

- The separator is under steady-state isothermal operation.
- Isobaric conditions.
- No radial concentration distributions in the tube or on the shell side of the reactor.
- Axial diffusion dispersion was neglected.

Ideal gas law is used to describe the gas behavior of single component and gas mixture with the assumptions specified above. The mass balance of component *i* can be written as:

Tube side (reaction side):

$$\frac{dF_i^t}{dz} = \frac{W}{V} A_{CS} \sum_{j=1}^{n} v_{i,j} r_j + \pi d_2 J_{O_2} \tag{4.1}$$

Shell side:

$$\frac{dF_{O_2}^s}{dz} = -\pi d_1 J_{O_2} \tag{4.2}$$

Since the membrane reactor for OCM is assumed to be operated under non-isothermal condition, the energy balance equation is involved for described the variance of reactor temperature. The energy balance of a tubular membrane reactor can be written as:

Tube side (reaction side):

$$\frac{dT^t}{dz} = \frac{[\frac{W}{V} A_{cs} \sum_i (-\Delta H_i r_i) - q + \pi d_2 J_{O_2} c_{p,O_2} \Delta T]}{\sum_j F_j C_{p_j}} \tag{4.3}$$

Shell side:

$$\frac{dT^s}{dz} = \frac{q}{F^s_{O_2} C_{p_{O_2}}} \tag{4.4}$$

where q is the heat flux between the tube side and shell side as expressed in the Equation (4.5). Table 4.1 gives the values of heat capacity of species j, Cp_j.

$$q = \frac{A_{cs} K_m (T^t - T^s)}{ML} \tag{4.5}$$

where A_{cs} is the cross section area of the tube side, K_m and M stand for the average thermal conductivity and membrane thickness, respectively, and L represents the effective length of the tube.

Table 4.1 Heat capacity of gas species involved in the reactions.

Species	**Cp_j (J/mol·K)**
CH_4	35.618
O_2	29.407
CO_2	37.144
H_2O	35.499
CO	28.517
C_2H_4	42.923
C_2H_6	52.623
H_2	28.869

4.3 Kinetics of oxidative coupling of methane

A comprehensive kinetic model of the OCM used in this study was developed by Stansch et al. (1997) for the La_2O_3/CaO catalyst. They proposed a reaction scheme for description of the network of primary reactions for the OCM involving all relevant chemical species. The reactions consist of three steps, which convert methane into ethane and other by-products, and seven consecutive reaction steps taking into account thermal gas phase dehydrogenation, heterogeneous catalytic oxidative dehydrogenation, ethylene steam reforming, and reaction inhibition by CO_2 and O_2. The kinetic model considered the following set of stoichiometric equation:

Step1: $CH_4+2O_2 \rightarrow CO_2+2H_2O$ $\Delta H°$=-802.251 kJ/mol (4.6)

Step2: $2CH_4+0.5O_2 \rightarrow C_2H_6+H_2O$ $\Delta H°$=-175.71 kJ/mol (4.7)

Step3: $CH_4+O_2 \rightarrow CO+H_2O+H_2$ $\Delta H°$=-277.449 kJ/mol (4.8)

Step4: $CO+0.5O_2 \rightarrow CO_2$ $\Delta H°$=-282.984 kJ/mol (4.9)

Step5: $C_2H_6+0.5O_2 \rightarrow C_2H_4+H_2O$ $\Delta H°$=-105.668 kJ/mol (4.10)

Step6: $C_2H_4+2O_2 \rightarrow 2CO+2H_2O$ $\Delta H°$=-757.156 kJ/mol (4.11)

Step7: $C_2H_6 \rightarrow C_2H_4+H_2$ $\Delta H°$=136.15 kJ/mol (4.12)

Step8: $C_2H_4+2H_2O \rightarrow 2CO+4H_2$ $\Delta H°$=210.116 kJ/mol (4.13)

Step9: $CO+H_2O \rightarrow CO_2+H_2$ $\Delta H°$=-41.166 kJ/mol (4.14)

Step10: $CO_2+H_2 \rightarrow CO+H_2O$ $\Delta H°$=41.166 kJ/mol (4.15)

The reaction rates for each step are given below:

$$r_j = \frac{k_{0,j} e^{-E_{a,j}/RT} P_C^{m_j} P_{O_2}^{n_j}}{(1 + K_{j,CO_2} e^{-\Delta H_{ad,CO_2}/RT} P_{CO_2})^2} \qquad j = 1, 3-6 \tag{4.16}$$

$$r_2 = \frac{k_{0,2} e^{-E_{a,2}/RT} (K_{0,O_2} e^{-\Delta H_{ad,O_2}/RT} P_{O_2})^{n_2} P_{CH_4}}{[1 + (K_{0,O_2} e^{-\Delta H_{ad,O_2}/RT} P_{O_2})^{n_2} + K_{j,CO_2} e^{-\Delta H_{ad,CO_2}/RT} P_{CO_2}]^2} \tag{4.17}$$

$$r_7 = k_{0,7} e^{-E_{a,7}/RT} P_{C_2H_6} \tag{4.18}$$

$$r_8 = k_{0,8} e^{-E_{a,8}/RT} P_{C_2H_4}^{m_8} P_{H_2O}^{n_8} \tag{4.19}$$

$$r_9 = k_{0,9} e^{-E_{a,9}/RT} P_{CO}^{m_9} P_{H_2O}^{n_9} \tag{4.20}$$

$$r_{10} = k_{0,10} e^{-E_{a,10}/RT} P_{CO_2}^{m_{10}} P_{H_2}^{n_{10}} \tag{4.21}$$

where P_i stands for the partial pressure of component i, K_0 and $E_{a,j}$ represent the kinetic parameter and the activation energy in reaction j, respectively. The kinetic parameters used for the above reaction scheme are presented in Table 4.2.

Table 4.2 Kinetic parameters of the OCM reactions (Stansch et al., 1997).

Step	$K_{0,j}$ (mol $g^{-1}s^{-1}Pa^{-(m+n)}$)	$E_{a,j}$ (kJ mol^{-1})	m_j	n_j	$K_{j,CO2}$ (Pa^{-1})	$\Delta H_{ad,CO2}$ (kJ mol^{-1})	$K_{j,O2}$ (Pa^{-1})	$\Delta H_{ad,O2}$ (kJ mol^{-1})
1	0.20×10^{-5}	48	0.24	0.76	0.25×10^{-12}	-175		
2	23.2	182	1.00	0.40	0.83×10^{-13}	-186	0.23×10^{-11}	-124
3	0.52×10^{-6}	68	0.57	0.85	0.36×10^{-13}	-187		
4	0.11×10^{-3}	104	1.00	0.55	0.40×10^{-12}	-168		
5	0.17	157	0.95	0.37	0.45×10^{-12}	-166		
6	0.06	166	1.00	0.96	0.16×10^{-12}	-211		
7	1.2×10^{7} [a]	226						
8	9.3×10^{3}	300	0.97	0				
9	0.19×10^{-3}	173	1.00	1.00				
10	0.26×10^{-1}	220	1.00	1.00				

[a]Units are mol $s^{-1}m^{-3}Pa^{-1}$.

4.4 Oxygen permeation rate of $Ba_{0.5}Sr_{0.5}Co_{0.8}Fe_{0.2}O_{3-\delta}$ tubular membrane

For the oxygen permeation through tubular BSCFO membrane, the oxygen flux Equation (4.22), which was developed by Kim et al. (1998), can be used to predict the permeation flux when a bulk diffusion is the controlling step for oxygen permeation. Lu et al. (2006) deduced the ambipolar diffusion coefficients D_a for the BSCFO material based on the bulk oxygen ionic diffusion current model. Table 4.3 presents the ambipolar diffusion coefficients D_a of the oxygen permeation fluxes of the BSCFO membrane at 700-900 °C.

$$J_{O_2} = \frac{\pi L C_i D_a}{2S \ln(d_1 / d_2)} \ln\left(\frac{P_1}{P_2}\right) \tag{4.22}$$

where d_1 and d_2 are the outer and inner diameter of the membrane tube, respectively, L , S, C_i and D_a stand for the effective length of the tube, the effective area of the membrane tube, the density of oxygen ions and the ambipolar diffusion coefficients, respectively, P_1 is the oxygen partial pressure in the shell side and P_2 is the oxygen partial pressure in the tube side.

Table 4.3 The ambipolar diffusion coefficients (D_a) at different temperature (700-900 °C) (Lu et al., 2006).

T (°C)	D_a (cm^2s^{-1})
700	0.77×10^{-6}
750	1.16×10^{-6}
800	1.68×10^{-6}
850	2.34×10^{-6}
900	3.31×10^{-6}

4.5 OCM performance

The main purpose of this study is to maximize the OCM process performance. The performance of membrane reactors in terms of CH_4 conversion (X_{CH4}) , C_2 selectivity (S_{C2}) and C_2 yield (Y_{C2}) is considered with respect to the effect of key operating parameters such as temperature, methane to oxygen feed ratio and methane feed flow rate. The above quantities are defined as follows:

$$X_{\mathrm{CH_4}}(\%) = \frac{\text{moles of } \mathrm{CH_4} \text{ converted}}{(\text{moles of } \mathrm{CH_4})_{\text{feed}}} \times 100 \tag{4.23}$$

$$S_{C_2}(\%) = \frac{2\times(\text{moles of } \mathrm{C_2} \text{ hydrocarbons})_{\text{products}}}{\text{moles of } \mathrm{CH_4} \text{ converted}} \times 100 \tag{4.24}$$

$$Y_{C_2}(\%) = \frac{2\times(\text{moles of } \mathrm{C_2} \text{ hydrocarbons})_{\text{products}}}{(\text{moles of } \mathrm{CH_4})_{\text{feed}}} \times 100 \tag{4.25}$$

4.6 Model validation

The validity of the kinetic model was tested by comparing the simulation results with experimental data for OCM reported by Stansch et al. (1997). Their experiments were operated in a plug flow reactor at a feed flow rate of 4 cm^3s^{-1} over 14.8 mg of La_2O_3/CaO catalyst. The comparison of the model prediction and experimental data in terms of CH_4 conversion (X_{CH4}) , C_2 selectivity (S_{C2}) and C_2 yield (Y_{C2}) at different feed mole ratio and operating temperatures is shown in Table 4.4. It can be seen that the model prediction shows good agreement with experimental data in the literature.

Table 4.4 Comparison between model prediction and experimental data (Stansch et al.,1997).

	Temperature (°C)				
	700	750	750	830	830
Feed mole ratio					
CH_4	0.699	0.612	0.699	0.612	0.699
O_2	0.095	0.051	0.095	0.051	0.095
X_{CH4} *(%)*					
Experimental	4.1	4.9	7.1	9.9	14.4
Simulated	4.5	4.8	6.5	12	13.8
S_{C2} *(%)*					
Experimental	35.6	55.6	53.7	72.5	69.6
Simulated	34.5	56.2	49.7	68.4	62
Y_{C2} *(%)*					
Experimental	1.5	2.7	3.8	7.2	10
Simulated	1.3	2.7	2.9	7.4	9.5

CHAPTER V

PERFORMANCE ANALYSIS OF MEMBRANE REACTOR FOR OXIDATIVE COUPLING OF METHANE

This chapter presents the simulation results of oxidative coupling of methane (OCM) in a single- and multi-stage membrane reactor. The effect of operating parameters studied which consists of methane to oxygen feed ratio (CH_4/O_2), operating temperature and methane feed flow rate are discussed.

5.1 A single-stage membrane reactor

In this section, the simulation results of a dense tubular membrane reactor for OCM process are presented. As earlier mentioned, a dense $Ba_{0.5}Sr_{0.5}Co_{0.8}Fe_{0.2}O_{3-\delta}$ membrane tube separates the reactor into the tube side where methane is fed and reacts with oxygen permeating through the membrane, and the shell side where oxygen (air) is fed. The La_2O_3/CaO catalyst is packed in the tube side. The value of simulated reactor dimensions and operational parameters is listed in Table 5.1.

5.1.1 Concentration profiles

The operating characteristics of membrane reactor for OCM process can be understood by examining its concentration profiles. The concentration profiles of CH_4, C_2, O_2, CO_x, H_2 and H_2O on the tube (reaction) side are shown in Figure 5.1. Pure methane is fed to the tube side at the rate of 1.6×10^{-3} mol/s. Methane and oxygen feeds are kept at a mole ratio of 2 and the operating temperature is constant at 800°C. It can be seen that methane concentration decreases along the reactor and the other gases start at zero and then increase due to the reactions occurred by permeated

oxygen from the shell side. In the early stage of the reactions, the formation rate of C_2 products by the OCM reactions is higher than the rate of methane undergoes deep oxidation (side reactions) as shown by the greater increase in the C_2 products concentration than that of the H_2, H_2O and CO_x gas.

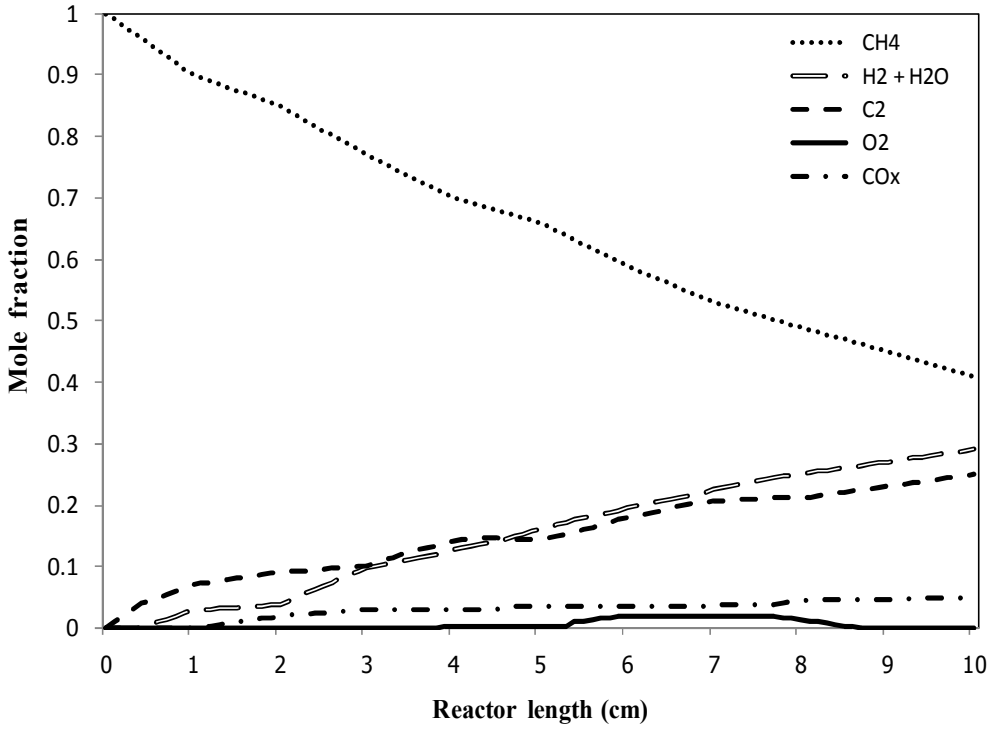

Figure 5.1 Concentration profiles at the reaction side of the membrane reactor.

Table 5.1 Operating conditions and reactor parameters.

Process Conditions	
Operating temperature (°C)	700-900 (800)
Methane/Oxygen feed ratio	0.5-3 (2)
Methane feed flow rate (10-3 mol/s)	1.2-2.8 (1.6)
Parameters	
Length (cm)	10
Inner diameter of membrane tube (mm)	5
External diameter of membrane tube (mm)	8
Mass of catalyst (g)	0.45
Pressure for both tube and shell sides (atm)	1
Bulk bed porosity	0.36

5.1.2 Effect of methane to oxygen feed ratio

In this section, the effect of methane to oxygen feed ratio on the performance of a single stage membrane reactor is analyzed. A number of simulations were carried out with varying CH_4/O_2 ratio from 0.5 to 3, the operating temperature is constant at 800°C and methane feed flow rate is fixed at 1.6×10^{-3} mol/s. This simulation results are shown in Figure 5.2. It can be seen that CH_4 conversion and C_2 yield were highest at CH_4/O_2 ratio of 0.5 and then decreased with increasing the CH_4/O_2 ratio due to the lower oxygen concentration in the reaction side. However, the undesired oxidation reaction of methane, C_2 products and other intermediate products were intensely induced at higher oxygen concentration, as a result, C_2 selectivity decreased at higher CH_4 conversion as well. Figure 5.3 shows the CH_4/O_2 ratio effect on the C_2H_4/C_2H_6 ratio in the C_2 products. Because the reaction of ethane to ethylene requires oxygen to react with ethane, higher C_2H_4/C_2H_6 ratio is obtained at lower CH_4/O_2 ratio. Since

C_2H_4 is more valuable than C_2H_6, operation with low CH_4/O_2 ratio is more suitable in terms of C_2 yield and C_2H_4/C_2H_6 ratio.

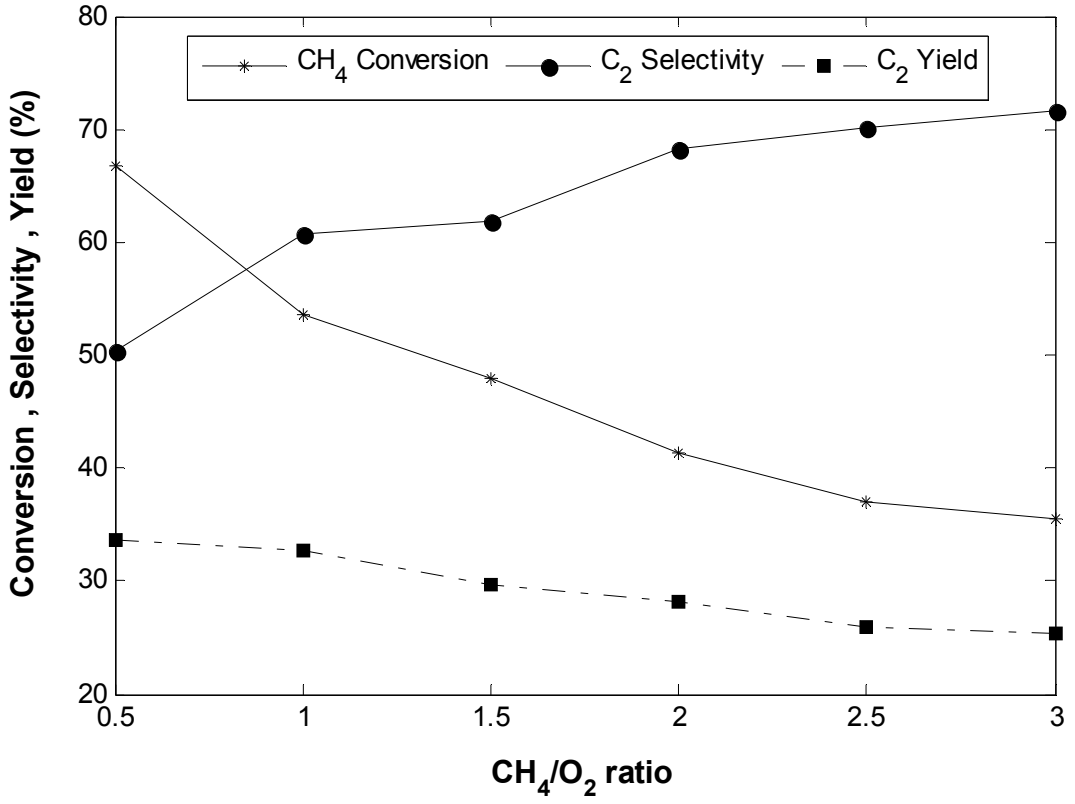

Figure 5.2 Effect of CH_4/O_2 ratio on the conversion of methane and the selectivity and yield of C_2 product**.**

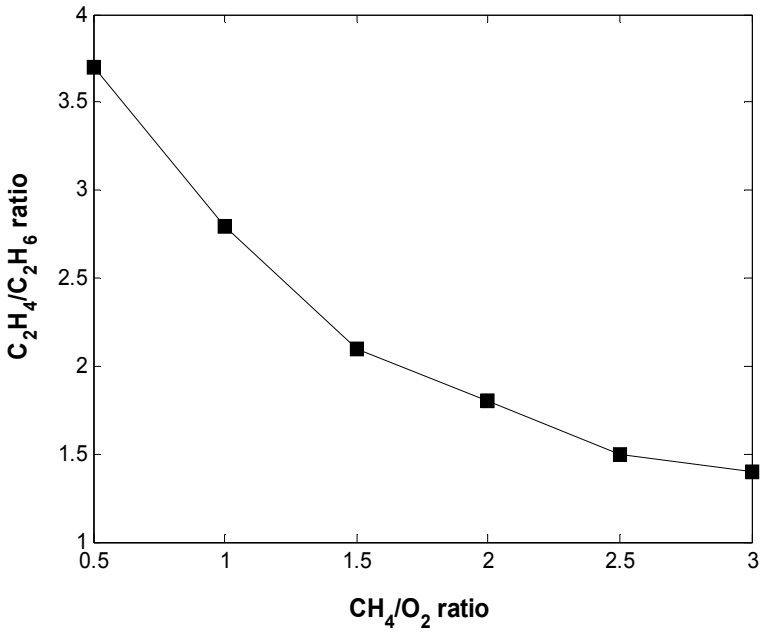

Figure 5.3 Effect of CH_4/O_2 ratio on the C_2H_4/C_2H_6 product ratio.

5.1.3 Effect of operating temperature

The effect of operating temperature on the performance of a single stage membrane reactor in OCM reaction is presented in Figure 5.4. Methane and oxygen are fed with a molar ratio of 2 and methane feed flow rate is fixed at 1.6×10^{-3} mol/s. The temperatures are considered in a range of 700-900 °C. Initially, the CH_4 conversion and C_2 product yield are increased with increasing operating temperature due to the higher reaction rate and oxygen flux through the membrane at higher temperature. At the temperature above 850 °C, however, the amount of methane in the tube side decreases, while the permeation of oxygen into the tube side increases. This leads to more undesired side reaction and causes a decrease in C_2 selectivity and C_2 yield. The increasing of H_2, H_2O and CO_x products indicated that hydrocarbons oxidation activity over La_2O_3/CaO catalyst is favored at high temperature. As a result, the C_2 selectivity is reduced with higher operating temperature. The increasing of C_2H_4/C_2H_6 ratio with an increase in temperature as shown in Figure 5.5 suggests that the dehydrogenation (thermal cracking) of ethane to ethylene is favored at higher temperature.

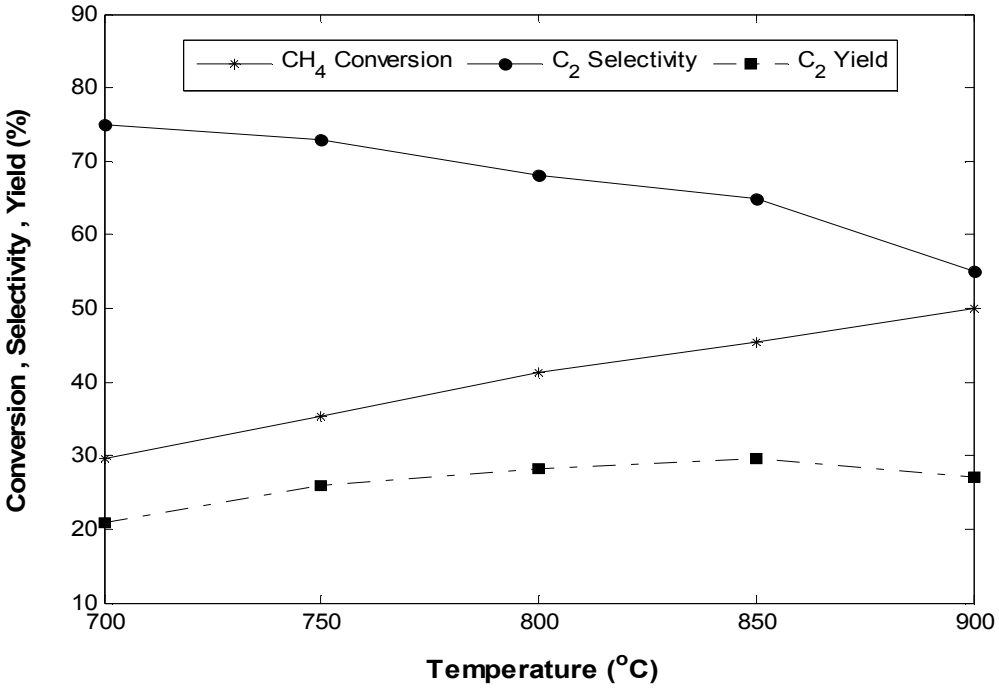

Figure 5.4 Effect of operating temperatures on the conversion of methane and the selectivity and yield of C_2 product.

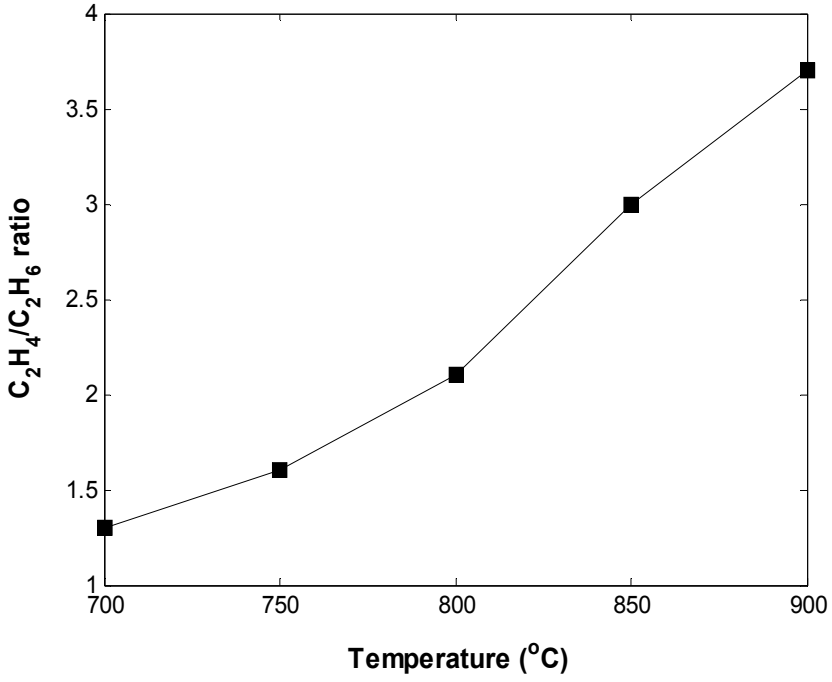

Figure 5.5 Effect of operating temperature on the C_2H_4/C_2H_6 product ratio.

5.1.4 Effect of methane feed flow rate

Figure 5.6 shows the variations of methane conversion, C_2 selectivity and yield of C_2 at different methane feed flow rate, while the operating temperature is constant at 800°C and methane to oxygen feed ratio of 2. The methane conversion, C_2 selectivity and C_2 yield improved initially and reaching maximum values at the methane feed flow rate of 2×10^{-3} mol/s. At methane feed flow rate below 2×10^{-3} mol/s, the performance of OCM process increases due to the rising chance of methane to react with oxygen. However, when the flow rate of methane over 2×10^{-3} mol/s, the oxygen concentration in the tube side is too little compared with methane concentration. As a result, the efficiency of OCM process decreases at higher methane feed flow rate. The trend is similar to the effect of methane feed flow rate on C_2H_4/C_2H_6 ratio as shown in Figure 5.7.

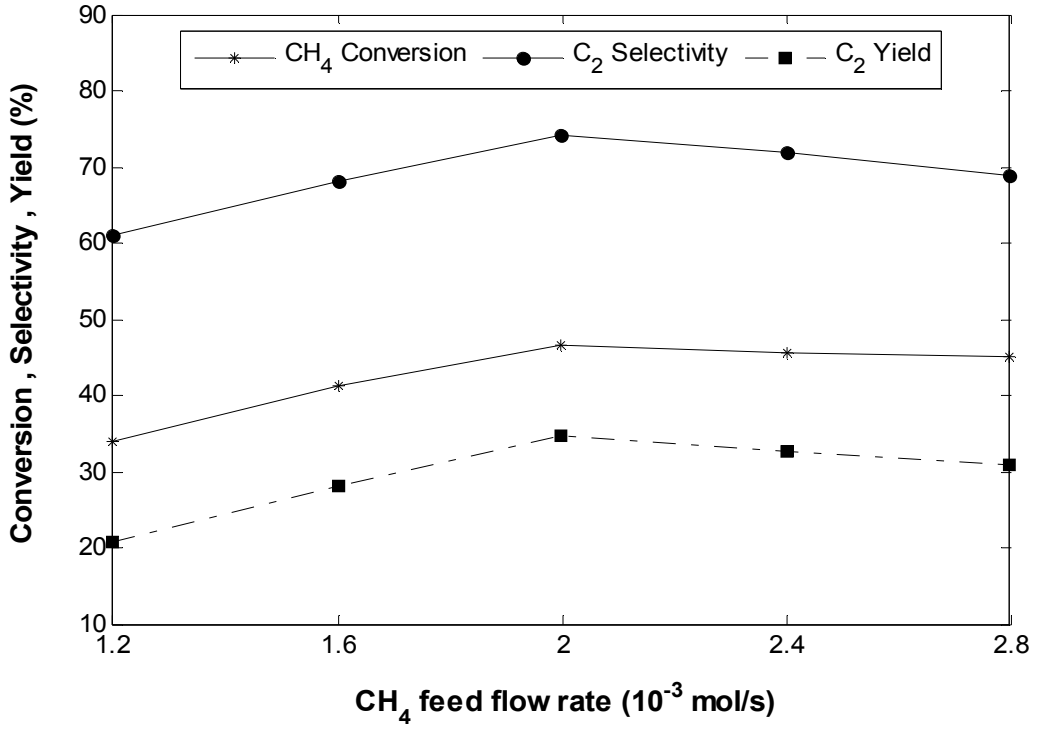

Figure 5.6 Effect of methane feed flow rate on the conversion of methane and the selectivity and yield of C_2 product.

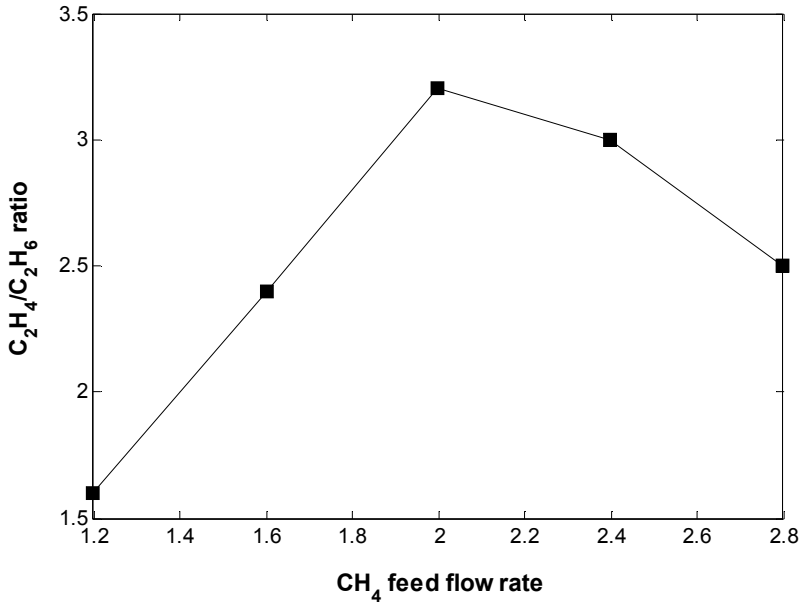

Figure 5.7 Effect of methane feed flow rate on the C_2H_4/C_2H_6 product ratio.

5.1.5 Adiabatic operation

Most of the simulation studies published in the literature on the OCM process in membrane reactors were based on mathematical models assuming isothermal condition. The assumption explained that the hot spot problem, that may be observed particularly with FBR, is less severe for the membrane reactors with the distributed oxygen supply along the reactors. Therefore, the reactors can be maintained at a nearly isothermal condition. However, due to the highly exothermic nature of OCM, isothermal assumption might lead to unrealistic prediction of the reactor performance. In this work, the effect of adiabatic operation is studied as well.

For OCM reaction, the increasing of operating temperature increases the reaction rates. Thus, the conversion of CH_4 and yield of C_2 are increased with an increase of temperature as shown in Section 5.1.3. In an adiabatic operation, heat released during oxidation coupling process increases the temperature as well as the rate of reactions. Figure 5.8 shows the temperature profile along the reactor under adiabatic operation with the inlet temperature of 700°C. It can be seen that the temperature increased along the reactor and reach to the highest temperature of

945.85°C. The effect of inlet temperature on the highest temperature and C_2 yield in each operation are presented in Figure 5.9. Both isothermal and adiabatic operation operate at the same process conditions as methane and oxygen are fed with a molar ratio of 2 and methane feed flow rate is fixed at 1.6×10^{-3} mol/s. It can be seen that C_2 yield with an adiabatic operation is higher than that in an isothermal operation at the inlet temperature range of 700-800 °C. The results are consistent with the results from earlier studies of the effect of operating temperature. Because of the low C_2 selectivity at high temperature, C_2 yield with an adiabatic operation is lower than that in an isothermal operation at the inlet temperature range of 850-900 °C.

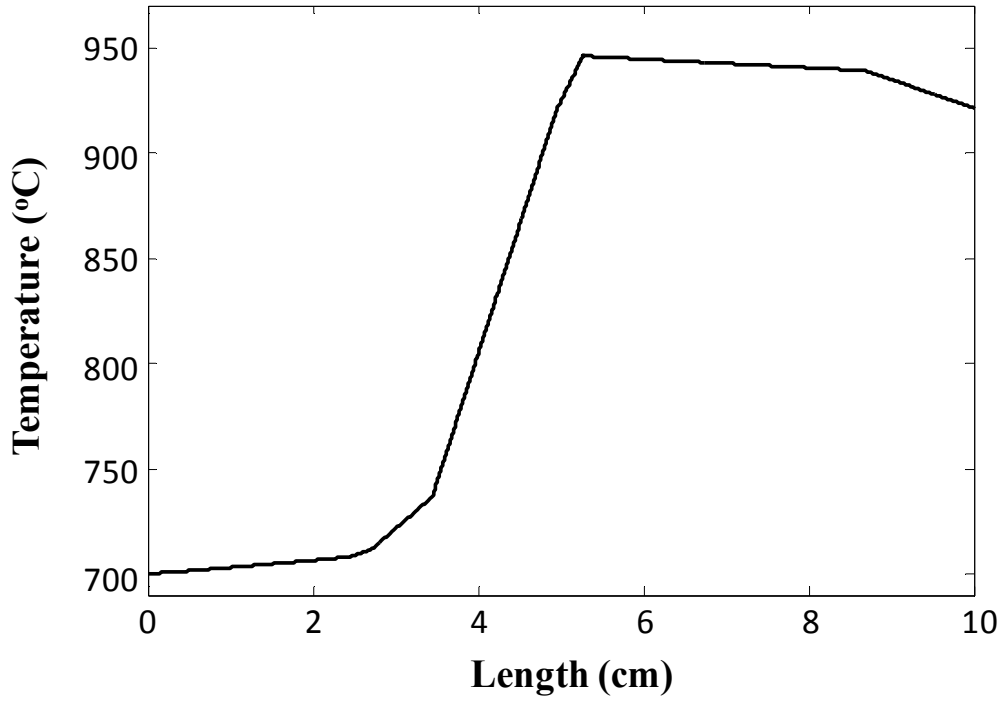

Figure 5.8 Temperature profile along the reactor.

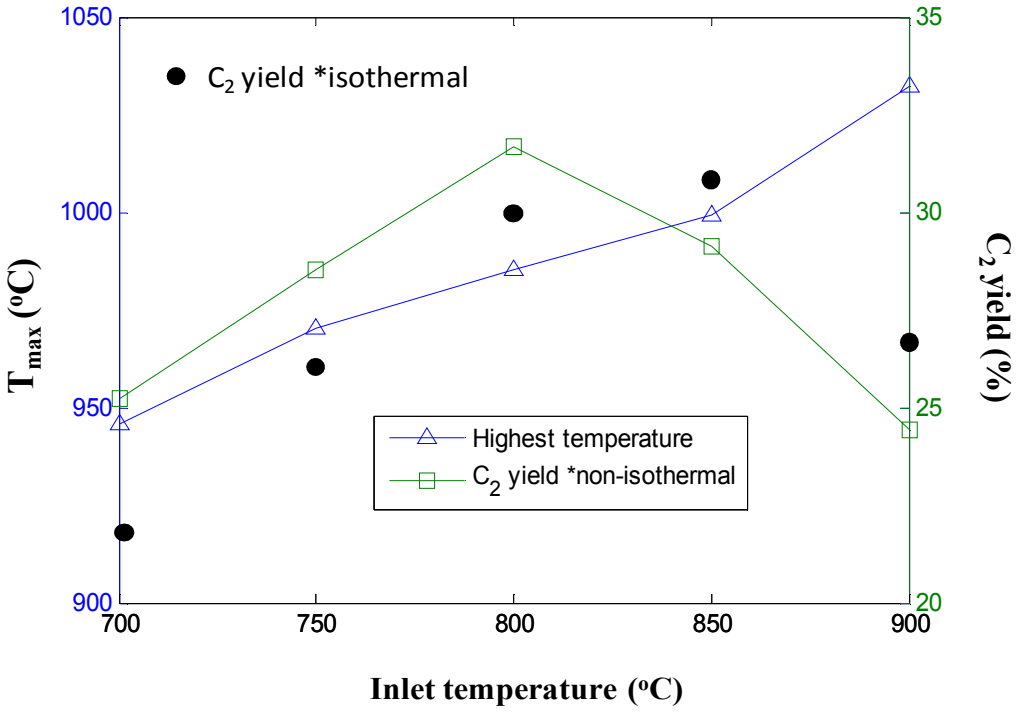

Figure 5.9 Effect of inlet temperatures on the highest temperature and C_2 yield of the membrane reactor operated under non-isothermal condition.

5.2 A multi-stage membrane reactor

In this section, the simulation results of a multi-stage membrane reactor for OCM process are presented. As earlier mentioned, three arrangements of oxygen feeding distribution are considered, i.e., increased feed (10-30-60 mol%), uniform feed (33-33-33 mol%) and decreased feed (60-30-10 mol%). The obtained results are shown in the subsequent section.

5.2.1 Oxygen concentration profile

Figure 5.10 shows the profiles of oxygen concentration at the tube side, which increases as more oxygen permeates from the shell side. Under the increased oxygen feeding policy, low oxygen content in the first stage of the multi-stage reactor can cause relatively low CH_4 conversion and C_2 yield. Higher permeated oxygen of the

decreased oxygen feeding policy affects to more CH_4 conversion than the other oxygen feeding distributions.

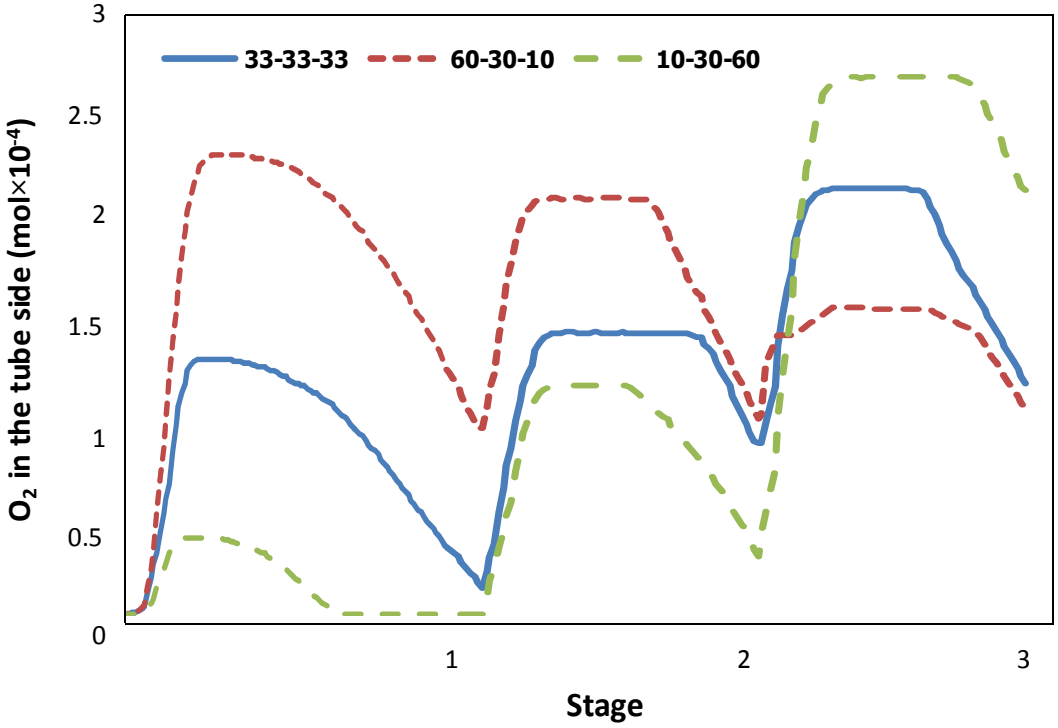

Figure 5.10 Concentration profile of oxygen at the tube side of membrane reactors**.**

5.2.2 Comparison of single- and multi-stage membrane reactors

5.2.2.1 Effect of methane to oxygen feed ratio

Figure 5.11 shows the effect of CH_4/O_2 ratio on the performance of single- and multi-stage membrane reactors. A number of simulations were carried out with varying CH_4/O_2 ratio from 0.5 to 3, the operating temperature is constant at 800°C and methane feed flow rate is fixed at 1.6×10^{-3} mol/s. It can be seen that the performance trend of the multi-stage membrane reactor with a decreased distribution of oxygen is quite similar to the single-stage membrane reactor and the performance of a decreased feed one is higher than that the single stage one in all terms. Therefore, this oxygen feeding pattern gives the appropriate amount of oxygen during the

reactions. The conversion of CH_4 and the yield of C_2 decrease with increasing the CH_4/O_2 ratio due to the lower oxygen concentration in the reaction side. The C_2 selectivity can be improved by using the multi-stage membrane reactor in all cases of oxygen feeding distribution, especially at high CH_4/O_2 ratio. In case of the multi-stage membrane reactor with increased feed of oxygen, due to the very low CH_4 conversion, the C_2 yield is therefore low even the highest C_2 selectivity is obtained.

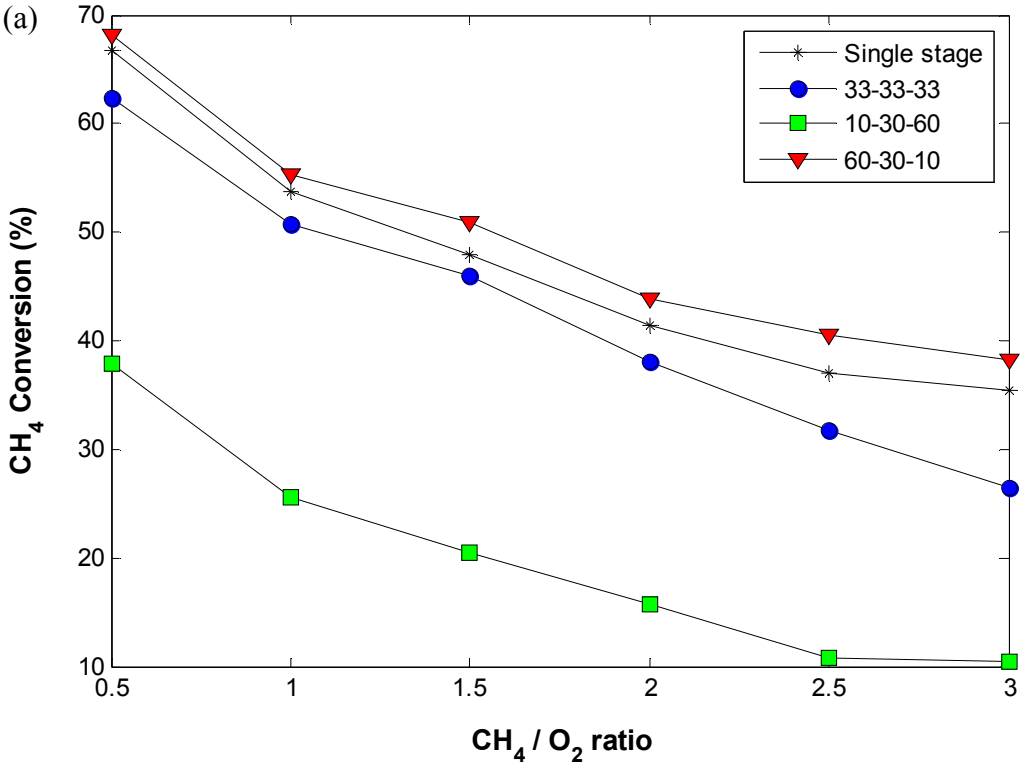

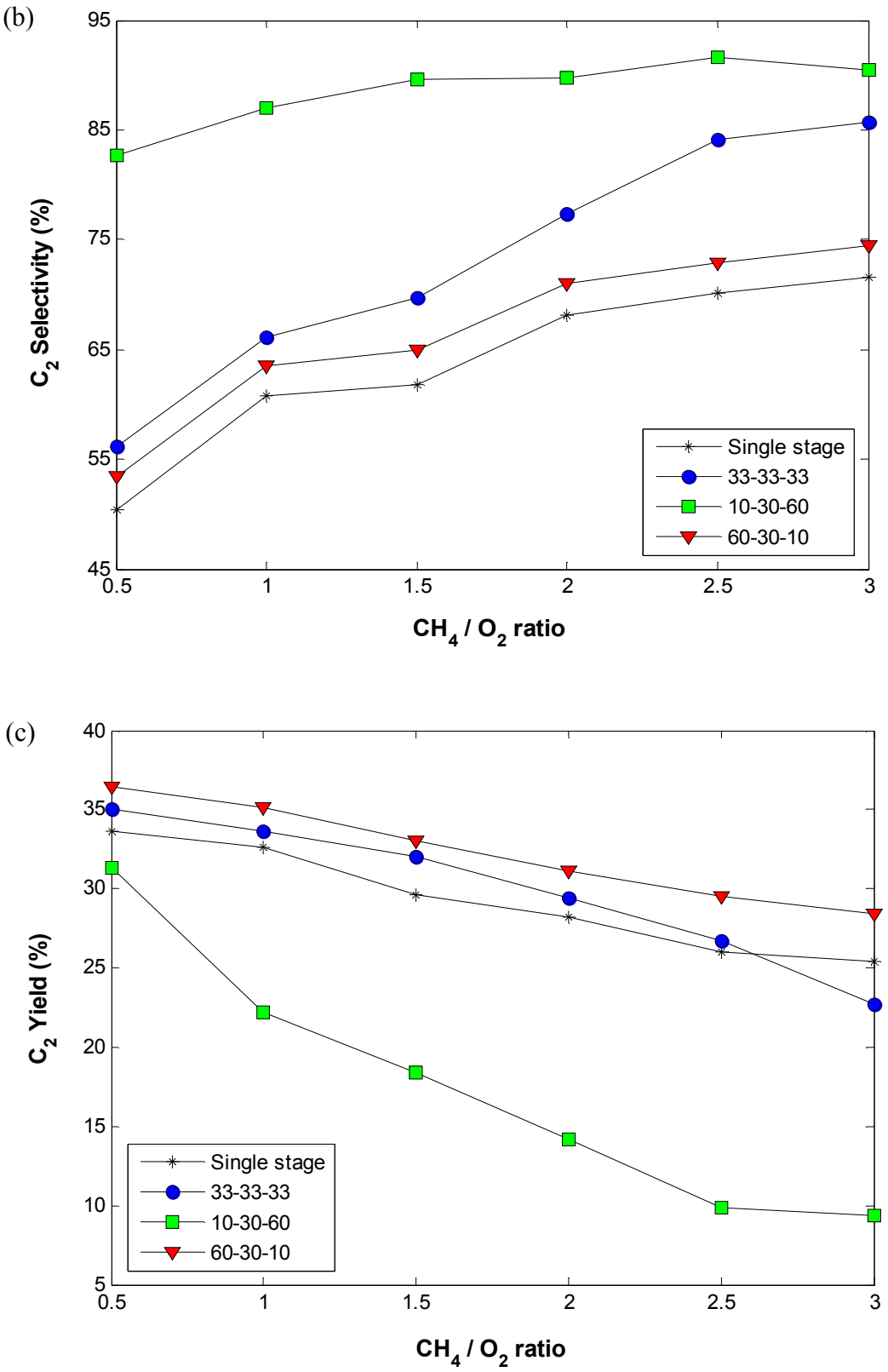

Figure 5.11 Effect of CH_4/O_2 ratio on single- and multi-stage membrane reactors**.**

5.2.2.2 Effect of operating temperature

The effect of operating temperatures on the performance of single- and multi-stage membrane reactors for the OCM reaction is presented in Figure 5.12. Methane and oxygen are fed with a molar ratio of 2 and methane feed flow rate is fixed at 1.6×10^{-3} mol/s. The temperatures are considered in a range of 700-900 °C. The conversion of methane in the single-stage membrane reactor is higher than that in the multi-stage reactor with uniform feed of oxygen, especially at the temperature higher than 750 °C, because of higher oxygen permeability. Methane conversion of a single-stage membrane reactor is lower than that of a multi-stage membrane reactor with decreased feed of oxygen because the permeated oxygen of a sigle stage one, which is higher than that of a multi-stage one, is used more in the side reactions than the main reactions. However, the C_2 selectivity of a single stage reactor is lower than a multi-stage reactor because a decrease in the methane partial pressure in the tube side leading to low methane and oxygen ratio (high oxygen content in the reaction side). It is found that the multi-stage membrane reactor operated under the uniform and decreased feeding policy of oxygen shows higher yield of C_2 than the single stage one. This is because a fine oxygen concentration in the reaction side leads to more C_2 selectivity than a single-stage membrane reactor.

(a)

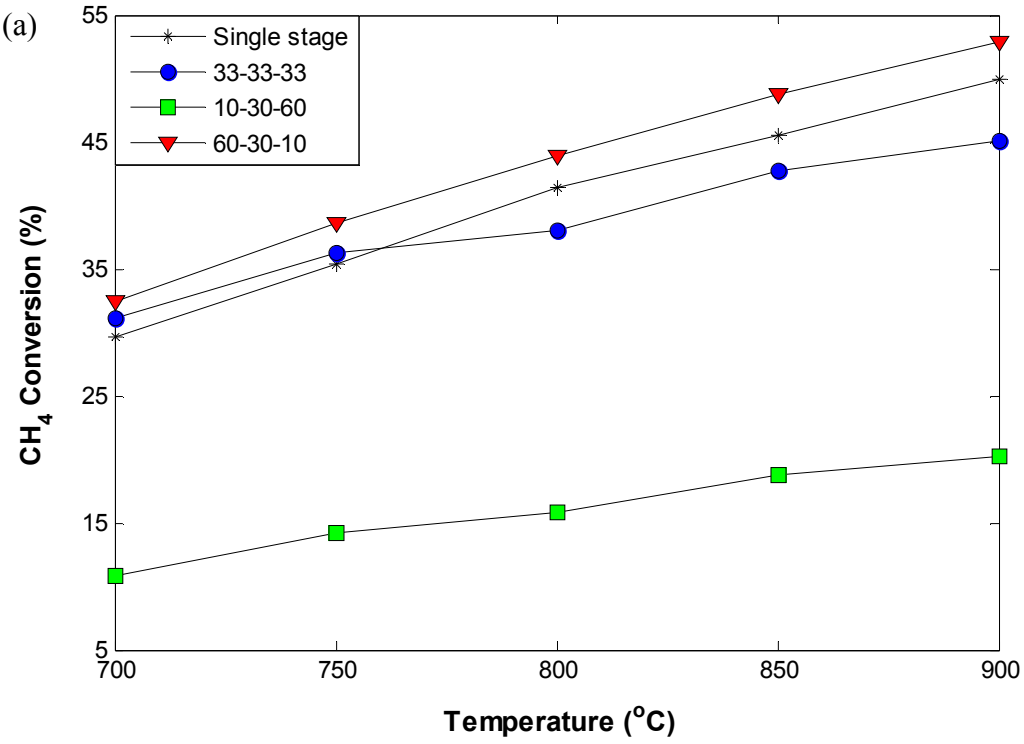
Single stage
33-33-33
10-30-60
60-30-10
CH4 Conversion (%)
Temperature (°C)
55
45
35
25
15
5
700
750
800
850
900

(b)

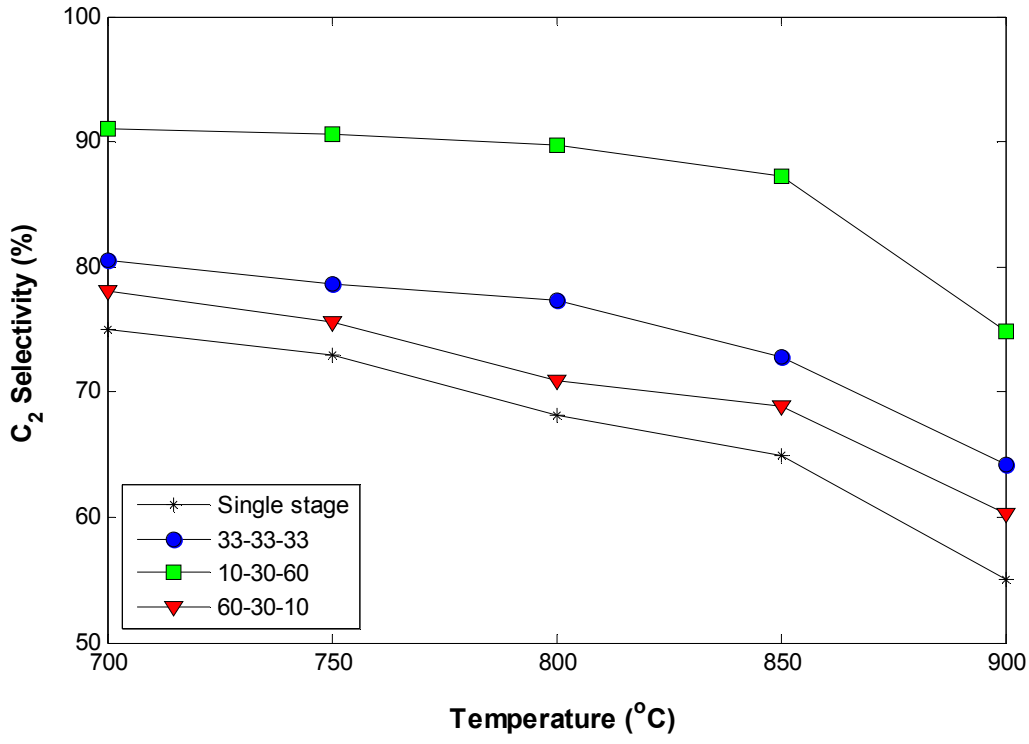
Single stage
33-33-33
10-30-60
60-30-10
C2 Selectivity (%)
Temperature (°C)
100
90
80
70
60
50
700
750
800
850
900

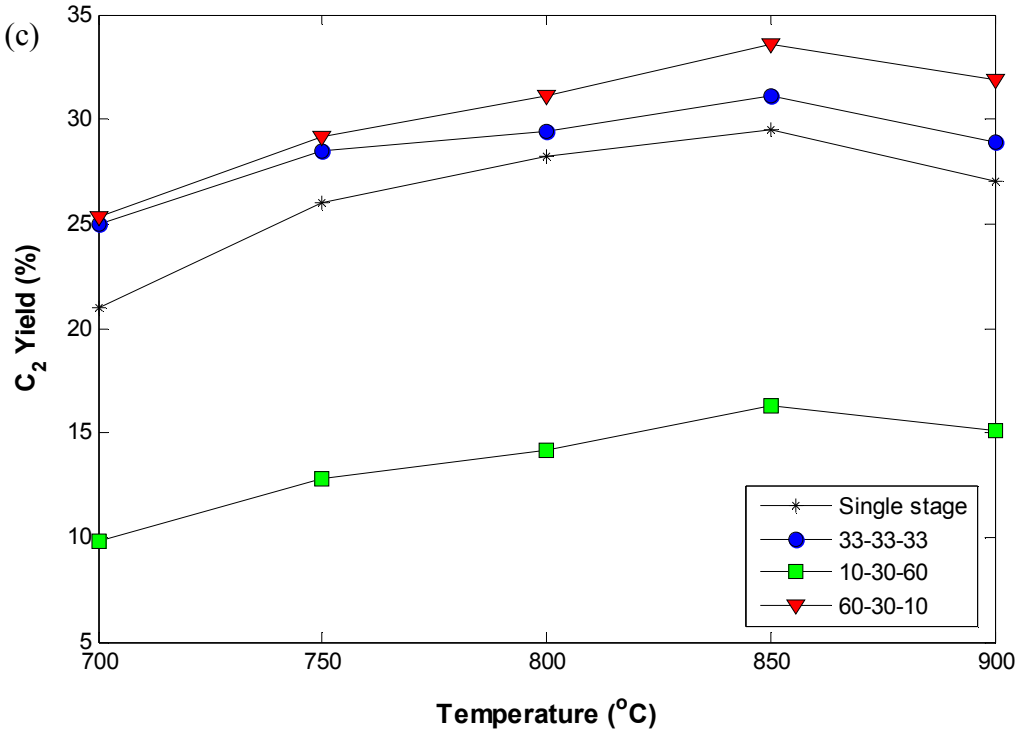

Figure 5.12 Effect of operating temperature on single- and multi-stage membrane reactors**.**

5.2.2.3 Effect of methane feed flow rate

Figure 5.13 shows the effect of methane feed flow rate on single- and multi-stage membrane reactors. The operating temperature is constant at 800°C and methane to oxygen feed ratio is equal to 2. Initially, the CH_4 conversion, C_2 selectivity and C_2 yield of the uniform and decreased feeding policy of oxygen increase with increasing methane feed flow rate, but those efficiency decreased as the methane feed flow rate over 2.4×10^{-3} mol/s. It is found that the multi-stage membrane reactor operated under the uniform and decreased feeding policy of oxygen shows higher yield of C_2 than the single stage one. CH_4 conversion and C_2 yield in case of the multi-stage membrane reactor with increased feed of oxygen are lowest compared with the others for all varying of operating parameters as shown in this section and the previous sections.

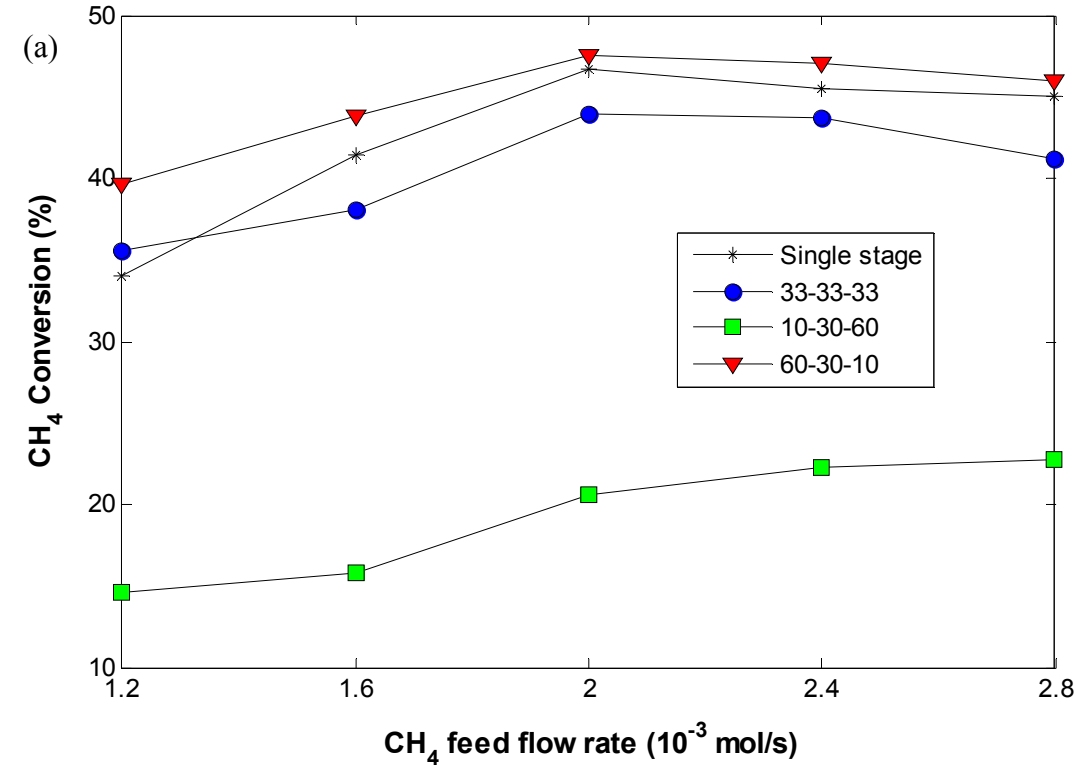
(a)
50
40
30
20
10
1.2
1.6
2
2.4
2.8
CH4 Conversion (%)
CH4 feed flow rate (10-3 mol/s)
Single stage
33-33-33
10-30-60
60-30-10

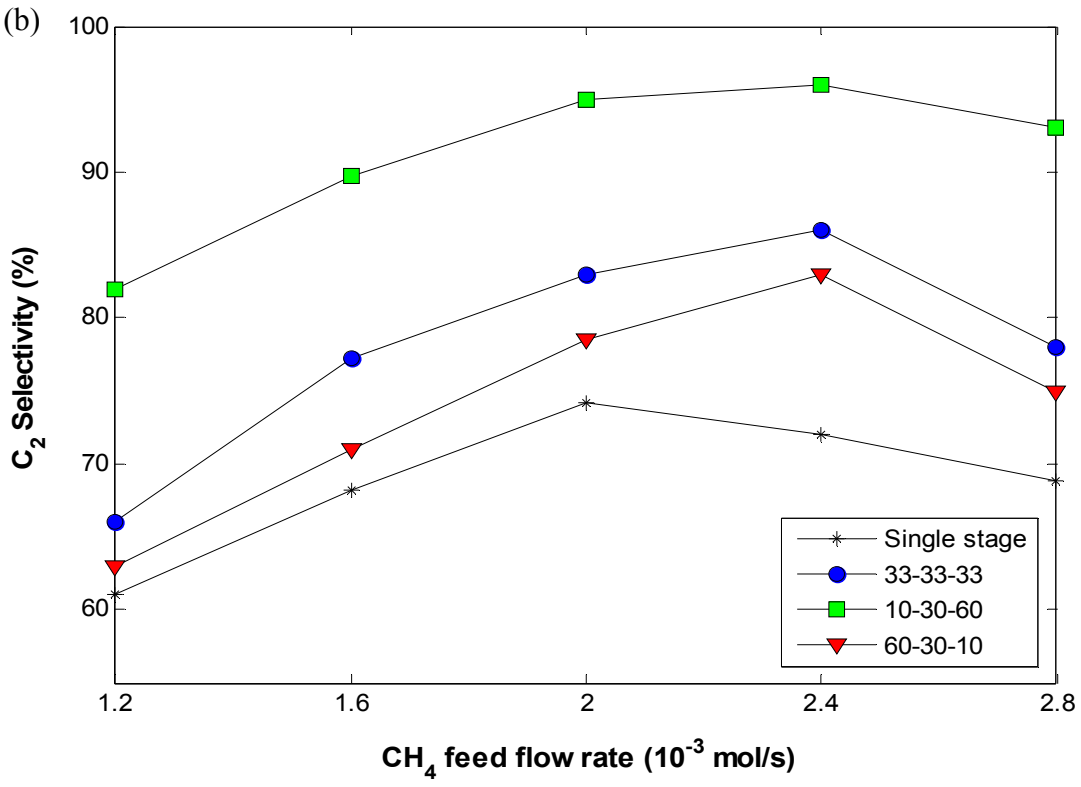
(b)
100
90
80
70
60
1.2
1.6
2
2.4
2.8
C2 Selectivity (%)
CH4 feed flow rate (10-3 mol/s)
Single stage
33-33-33
10-30-60
60-30-10

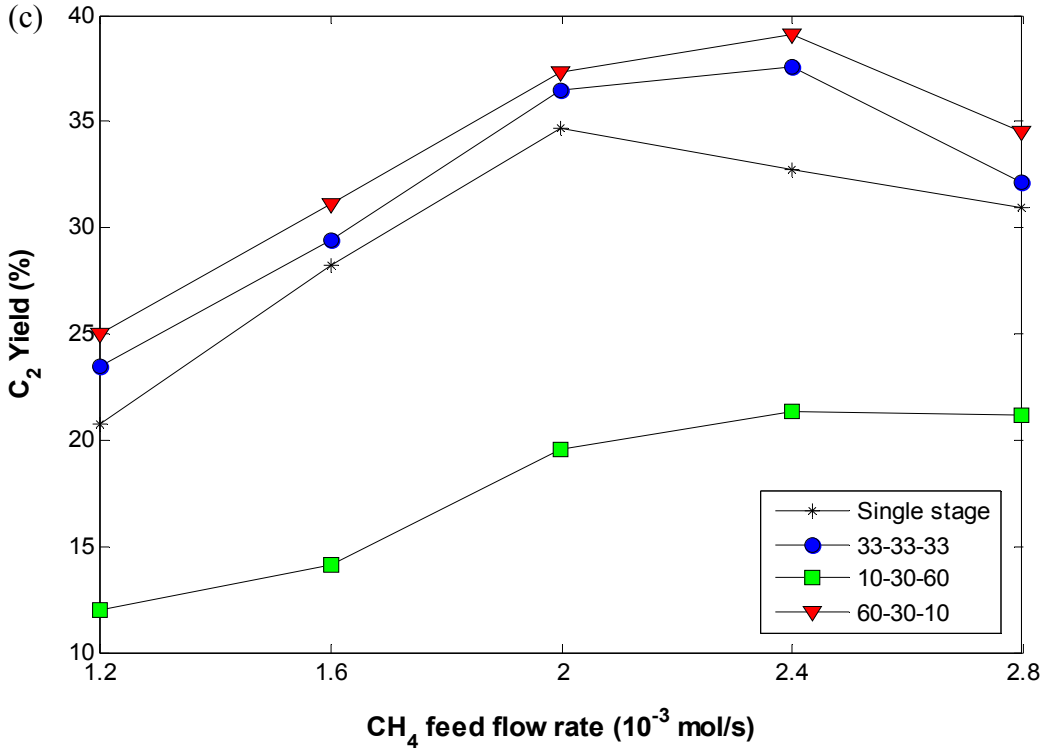

Figure 5.13 Effect of methane feed flow rate on single- and multi-stage membrane reactors**.**

5.2.3 Effect of decreased oxygen feed with different proportions

From the previous section, it can be seen that a multi-stage membrane reactor with decreased feed of oxygen give the highest C_2 yield. Thus, this section is focused on the decreased feed of oxygen with different proportions. Figure 5.14 shows the C_2 yield in case of decreased feed of oxygen with different proportions, i.e., 80-10-10, 70-20-10, 60-30-10 and 50-30-20 (mol%). Methane and oxygen are fed with a molar ratio of 2 and methane feed flow rate is fixed at 1.6×10^{-3} mol/s. The operating temperatures are considered in a range of 700-900 °C. It can be seen that the proportion of oxygen at each stage as 50-30-20 show a higher C_2 yield than the others. The result may be used as a guideline for the determination of appropriate amount of oxygen entering in each stage of the reactors. Half of the total amount of oxygen is fed in the first stage and then entering the next stage with half of the amount of oxygen in previous stage, and so on.

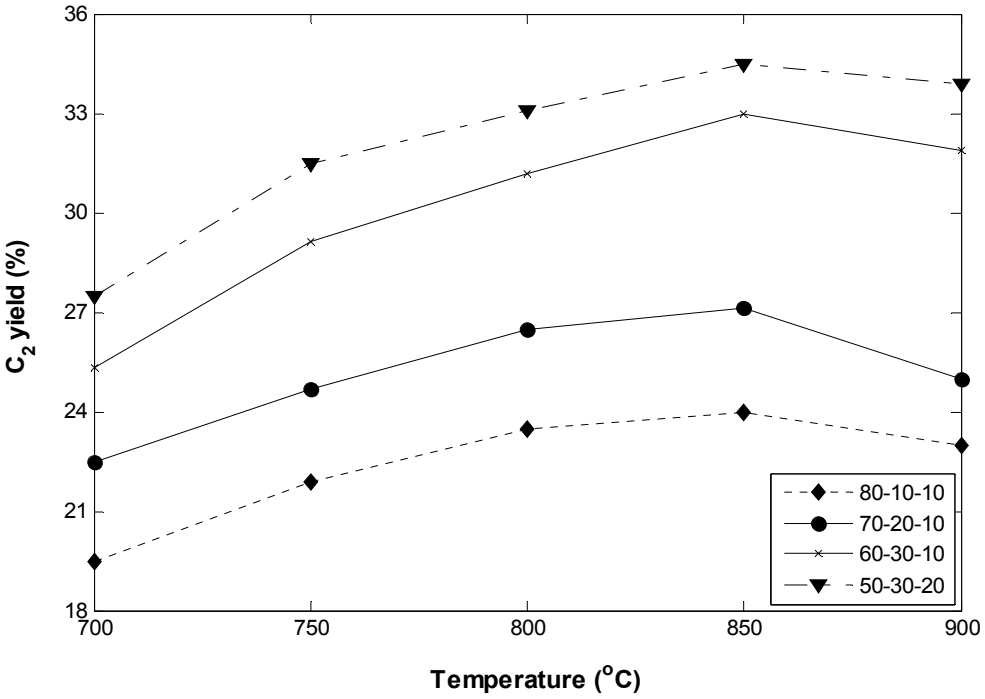

Figure 5.14 C_2 yield of the multi-stage membrane reactor with decreased feed of oxygen.

5.2.4 Adiabatic operation

This section presents the study of multi-stage membrane reactor in an adiabatic operation. The temperature profile of single- and multi-stage membrane reactor are shown in Figure 5.15. It can be seen that the rate of increase in temperature of a multi-stage membrane reactor is less than that of a single-stage one due to the lower occurrence of side reactions, which are highly exothermic reactions. In case of a multi-stage membrane reactor with increased feed of oxygen has the lowest temperature because of the higher C_2 selectivity or minimal side reactions.

When comparing the yield of C_2 products of isothermal and adiabatic conditions, the results are the same as the case of a single stage membrane reactor. The C_2 yield with an adiabatic operation is higher than that in an isothermal operation at the inlet temperature range of 700-800 °C, while C_2 yield with an adiabatic operation is lower than that in an isothermal operation at the inlet temperature range of 850-900 °C as shown in Figure 5.16.

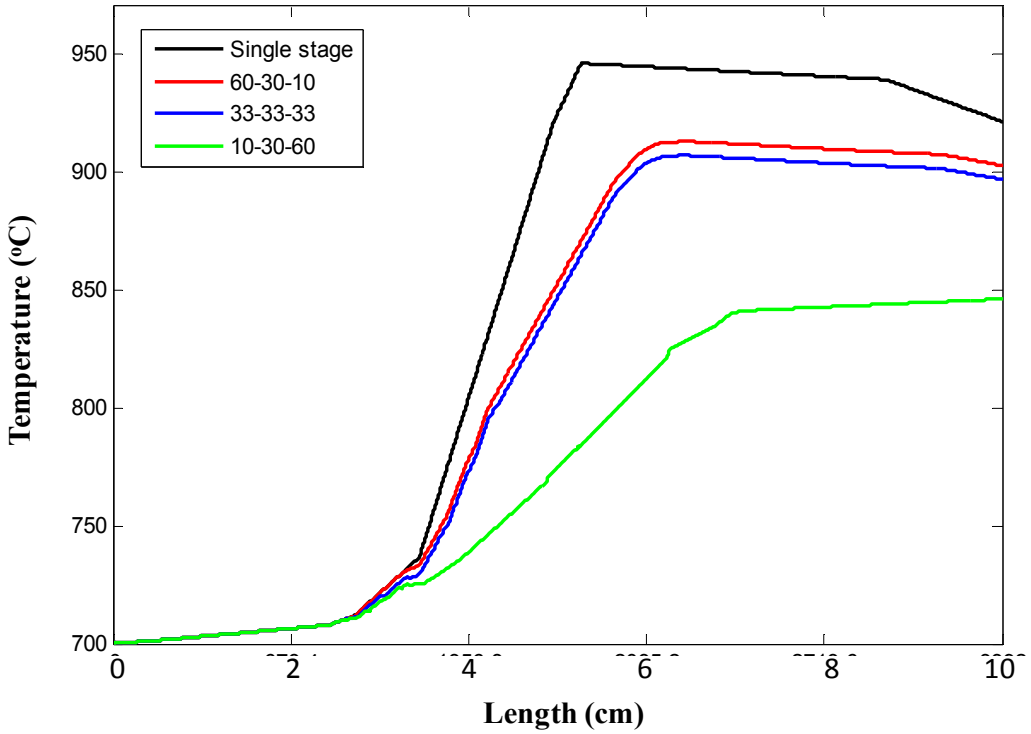

Figure 5.15 Temperature profile along single- and multi-stage membrane reactor.

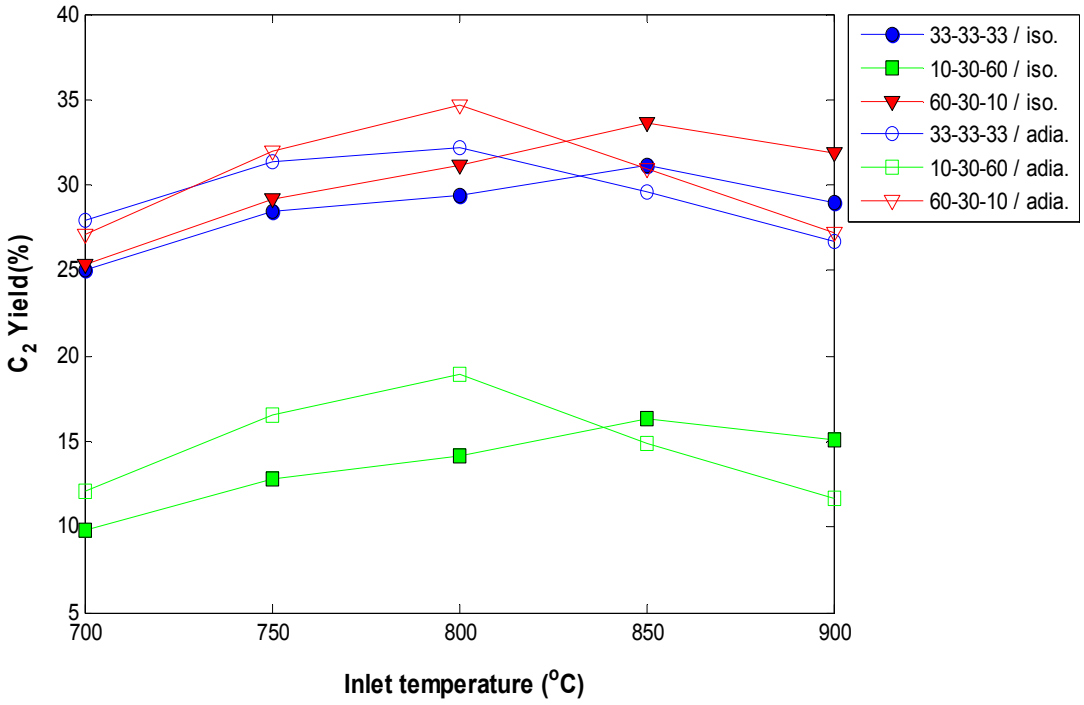

Figure 5.16 Effect of inlet temperature on the C_2 yield of a multi-stage membrane reactor operated under isothermal and adiabatic conditions.

CHAPTER VI

OPTIMIZATION OF MEMBRANE REACTOR FOR OXIDATIVE COUPLING OF METHANE

This chapter presents a study on determination of the optimal operating conditions for OCM process using the response surface methodology (RSM). RSM is a method that mainly involves three major steps: design of experiment using statistical approach, estimation of coefficient based on mathematical model and response prediction, and finally confirmation of model respectability.

6.1 Design of experiment

In this study, a statistical analysis of the OCM process performance in term of C_2 yield was performed using Design Expert software version 8.0.6.1 (STAT-EASE Inc., Minneapolis, USA). The central composite design (CCD) was used to study the interaction of process variables and to predict the optimum process conditions for maximize the C_2 products yield. The independent variables with the operating range of each variable are given in Table 6.1.

Table 6.1 Experimental range and levels of independent process variables for OCM.

Independent variable	Symbol	Coded levels		
		-1	0	1
CH_4/O_2 feed ratio	X_1	1	2	3
Operating temperature (°C)	X_2	700	800	900
CH_4 feed flow rate (10^{-3} mol/s)	X_3	1.2	2.0	2.8

The low (-1), middle (0) and high (1) levels for all independent variables were based on the previous chapter study and prior screening from the literature. The values shown in Table 6.1 are for CH_4/O_2 feed ratio, operating temperature and CH_4 feed flow rate. CH_4/O_2 feed ratio of 1, 2 and 3 were chosen for variable X_1; operating temperature at 700, 800 and 900°C for X_2 and 1.2, 2.0 and 2.8 (10^{-3} mol/s) for X_3. All variables at zero level constitute to the center points while combination of variables at star points, which consist of its lowest (-α) level or highest (+α) level, with other variables at zero level constitutes the axial points.

According to CCD, the total experiment combinations can be calculated using the following equation:

$$\text{The total number of experiments} = 2^n + 2n + n_0 \tag{6.1}$$

where n is the number of independent variables and n_0 is the number of replications at center point. In this study, n_0 is performed one because the result does not change in simulation method. Thus, a set of 15 experiments including the 8 factorial experiments, 6 star points and 1 center point were carried out. The distance of the star points from the center point is given by $\alpha = 2^{n/4}$ and equal to ±1.682 in this study. The complete design matrix of CCD and the simulation results are given in Table 6.2. The percentage of C_2 yield was taken as the response of the design experiment.

The response (Y) of the OCM process was used to develop a quadratic polynomial equation that correlates the C_2 production as a function of the independent variables and their interactions as shown in the Equation (6.2).

$$Y = \beta_0 + \sum_{i=1}^{3} \beta_i X_i + \sum_{i=1}^{3} \beta_{ii} X_i^2 + \sum_{i=1}^{2} \sum_{j=i+1}^{3} \beta_{ij} X_i X_j \tag{6.2}$$

where Y is the predicted response (dependent variables), β_0 is the offset term, β_i, β_{ii} and β_{ij} are coefficients for the linear, squared and interaction effects, respectively while X_i and X_j are factors (independent variables).

Table 6.2 Full factorial central composite design matrix of three independent variables in coded and unit along with the simulated response value

Run	Manipulated variables						Responses
	X_1		X_2		X_3		C_2 yield (%)
	CH_4/O_2 ratio	Level	Temperature	Level	CH_4 feed flow rate	Level	
1	1	-1	700	-1	1.2	-1	18.84
2	1	-1	700	-1	2.8	1	22.55
3	1	-1	900	+1	1.2	-1	32.55
4	1	-1	900	+1	2.8	1	32.56
5	3	1	700	-1	1.2	-1	11.59
6	3	1	700	-1	2.8	1	17.23
7	3	1	900	+1	1.2	-1	15.34
8	3	1	900	+1	2.8	1	21.23
9	0.32	-α	800	0	2.0	0	34.12
10	3.68	+α	800	0	2.0	0	13.78
11	2	0	631.82	-α	2.0	0	13.12
12	2	0	968.18	+α	2.0	0	27.32
13	2	0	800	0	0.65	-α	21.33
14	2	0	800	0	3.35	+α	29.12
15	2	0	800	0	2.0	0	31.41

6.2 Optimization of single-stage membrane reactor

6.2.1 Regression model equation for C_2 yield

Simulations of a single-stage membrane reactor for OCM process are performed based on the operating conditions as listed in Table 6.2. The results show that the C_2 yield is obtained varied from 11.59% to 34.12%, depending on the operating conditions. These results can be fitted by a second order quadratic model as given in Equation (6.3):

$$\begin{aligned} Y = & -330.594 + 19.779X_1 + 0.773X_2 + 20.031X_3 \\ & - 0.020X_1X_2 + 1.220X_1X_3 - (5.391\times10^{-3})X_2X_3 \\ & - 2.941X_1^2 - (4.260\times10^{-4})X_2^2 - 3.891X_3^2 \end{aligned} \tag{6.3}$$

From the equation, the yield of C_2 has linear and quadratic effects by the three process variables. This validation of the model obtained is shown by the R^2 error of 0.9888 or 98.88% of the response variability could be explained by this regression model. The value of R^2 is unity which means a complete agreement between predicted and actual responses. Figure 6.1 summarizes correlation between simulated values versus predicted values by using the developed model.

Statistical analysis based on ANOVA for the quadratic model developed by the software is shown in Table 6.3. The model F-value of 49.00 implies the model is significant. There is only a 0.02% chance that a "Model F-value" this large could occur due to noise. P-value less than 0.0500 indicate model terms are significant. In this case X_1, X_2, X_3, X_1X_2, X^2_1, X^2_2, X^2_3 are significant model terms. P-values greater than 0.1000 indicate the model terms are not significant. If there are many insignificant model terms (not counting those required to support hierarchy), model reduction may improve this model.

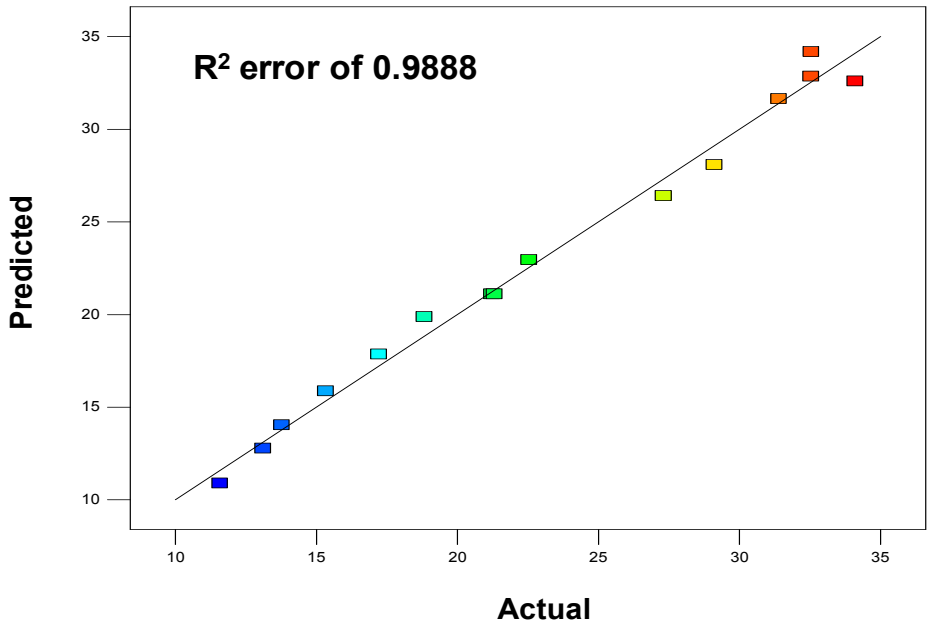

Figure 6.1 Predicted and actual values of C_2 yield for single-stage membrane reactor.

Table 6.3 ANOVA of the response surface quadratic model for single-stage membrane reactor.

Source	**SS**[a]	**DF**[b]	**MS**[c]	**F-value**	**P-value**
Model	851.09	9	94.57	49.00	0.0002
X_1	415.38	1	415.38	215.24	<0.0001
X_2	224.34	1	224.34	116.25	0.0001
X_3	58.86	1	58.86	30.50	0.0027
X_1X_2	31.88	1	31.88	16.52	0.0097
X_1X_3	7.62	1	7.62	3.95	0.1036
X_2X_3	1.49	1	1.49	0.77	0.4201
X^2_1	52.36	1	52.36	27.13	0.0034
X^2_2	109.83	1	109.83	56.91	0.0006
X^2_3	37.54	1	37.54	19.45	0.0070
Residual	9.65	5	1.93		
Total	860.74	14			

[a] SS = Sum of squares, [b] DF = Degree of freedom, [c] MS = Mean square

Std. Dev.	1.39	R-Squared	0.9888
Mean	22.81	Adj R-Squared	0.9686
C.V. %	6.09	Pred R-Squared	0.4989
PRESS	431.34	Adeq Precision	20.531

The "Pred R-Squared" of 0.4989 is not as close to the "Adj R-Squared" of 0.9686 as one might normally expect. This may indicate a large block effect or a possible problem with this model and/or data. Things to consider are model reduction, response transformation, outliers, etc. "Adeq Precision" measures the signal to noise ratio. A ratio greater than 4 is desirable. This ratio of 20.531 indicates an adequate signal. This model can be used to navigate the design space.

6.2.2 Results

The regression model (Equation (6.3)) can be used to map empirically the response function over the experimental region. The contour plot helps to evaluate the effect of any two independent variables combined on the response. Each contour curve represents an infinite number of responses of two process variables. The maximum predicted response is indicated by the surface confined in the smallest ellipse in the contour diagram.

In general, several 2-dimensional plots can provide some information on the effect of main process variables in chemical reactions. Unfortunately, most of chemical reactions, the reactor can be operated differently at different levels of process variables. Thus, it is often difficult to make any conclusions on the overall behavior of the system in the ranges of process variables as a number of 2-dimensional plots should be plotted and compared. In this particular respect, a 3-dimensional plots can present the overall behavior in a better way. Therefore, instead of individual 2-dimensional plots, it is believed that any possible interactions between the process variables should be more visible if a 3-dimensional plots are established from the experimental data.

6.2.2.1 Effect of one factor

The effect of CH_4/O_2 ratio, temperature and CH_4 feed flow rate on C_2 yield in case of a single-stage membrane reactor as shown in Figure 6.2. The trend of the results from the regression model predictions are consistent with the results of the simulation studies in previous chapter. When considering the variable that can affect C_2 yield the most by comparing its p-value, CH_4/O_2 ratio is that variable due to the lowest p-value of <0.0001.

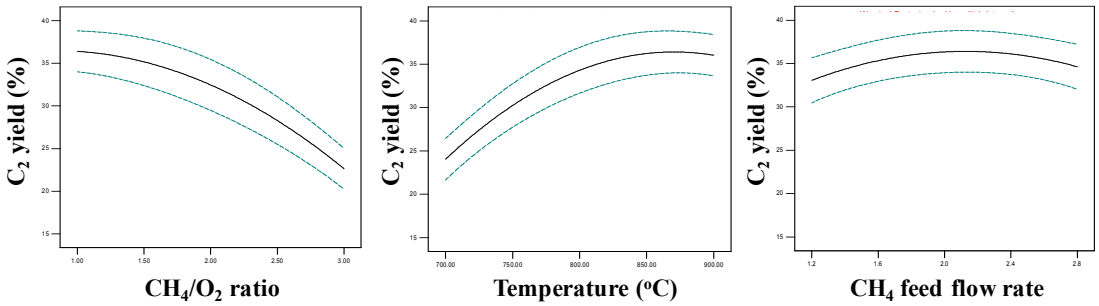

Figure 6.2 Effect of CH_4/O_2 ratio, temperature and CH_4 feed flow rate on C_2 yield in case of a single-stage membrane reactor.

6.2.2.2 Effect of an interaction between two variables

Figures 6.3 and 6.4 demonstrate the contour surface plot and the response surface 3D plot indicating the effect of interaction between CH_4/O_2 ratio and operating temperature on C_2 yield, respectively. It is noticed that for a decreasing of CH_4/O_2 ratio, the C_2 yield increased with increasing operating temperature. The observed phenomenon occurred as increasing the operating temperature enhanced the reaction rate of OCM reaction, as a result, high CH_4 conversion received and eventually the yield of C_2 products. On the other hand, the same trend was not applicable for CH_4/O_2 ratio because the too little oxygen concentration in the reaction side led to low CH_4 conversion and C_2 yield.

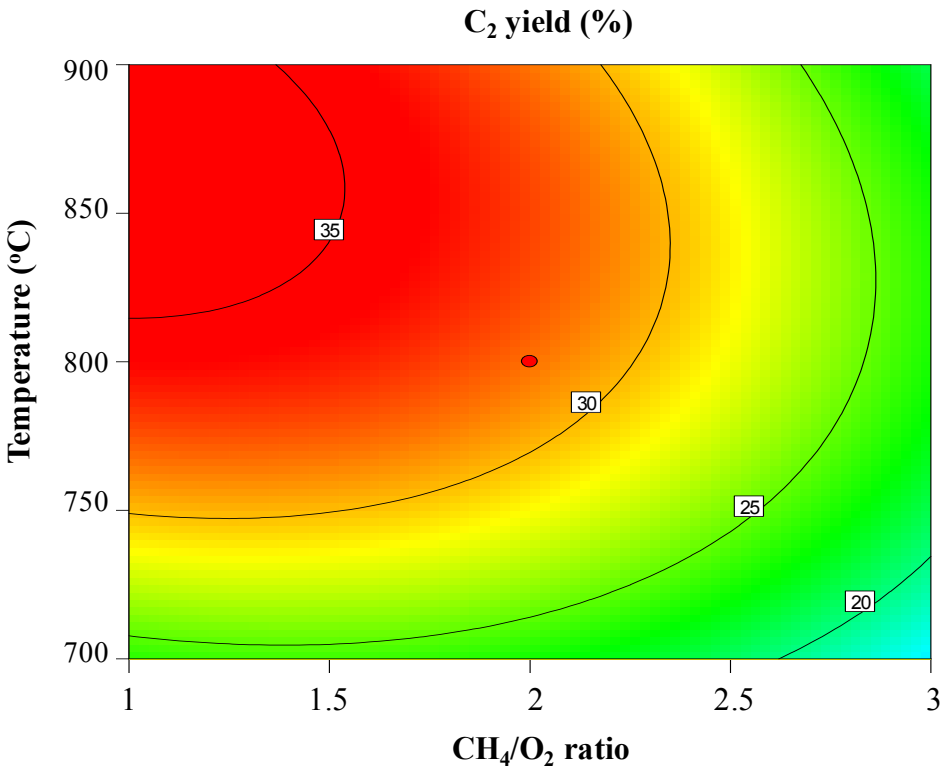

Figure 6.3 Contour surface plot of C_2 yield as a function of CH_4/O_2 ratio and operating temperature.

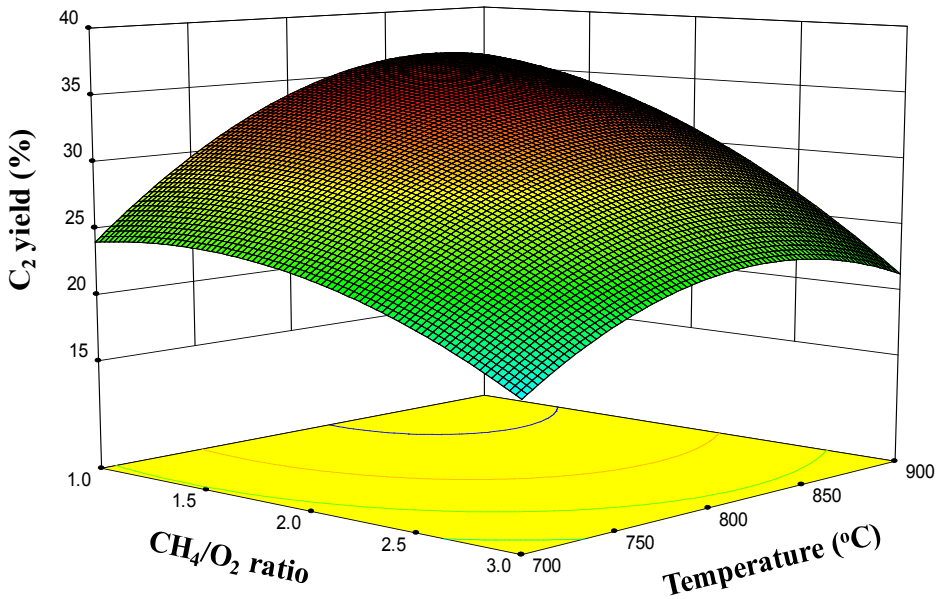

Figure 6.4 3-D graphic surface optimization of C_2 yield versus CH_4/O_2 ratio and operating temperature.

Figures 6.5 and 6.6 illustrate the contour surface plot and the response surface 3D plot indicating the effect of interaction between CH_4/O_2 ratio and CH_4 feed flow rate on C_2 yield, respectively. The optimum response value can be clearly observed from the contour plot. By analyzing the plots, the optimal conditions obtained for C_2 yield were 1-2 of CH_4/O_2 ratio and 1.6-2.7 (10^{-3} mol/s) of CH_4 feed flow rate.

Figures 6.7 and 6.8 present the contour surface plot and the response surface 3D plot indicating the effect of interaction between operating temperature and CH_4 feed flow rate on C_2 yield, respectively. By analyzing the plots, the optimal conditions obtained for C_2 yield were the operating temperature of 800-900°C and 1.8-2.8 (10^{-3} mol/s) of CH_4 feed flow rate.

When considering the interaction between two variables that can affect C_2 yield the most by comparing its p-value, the interaction between CH_4/O_2 ratio and operating temperature shows the most affect to C_2 yield due to the lowest p-value of 0.0097.

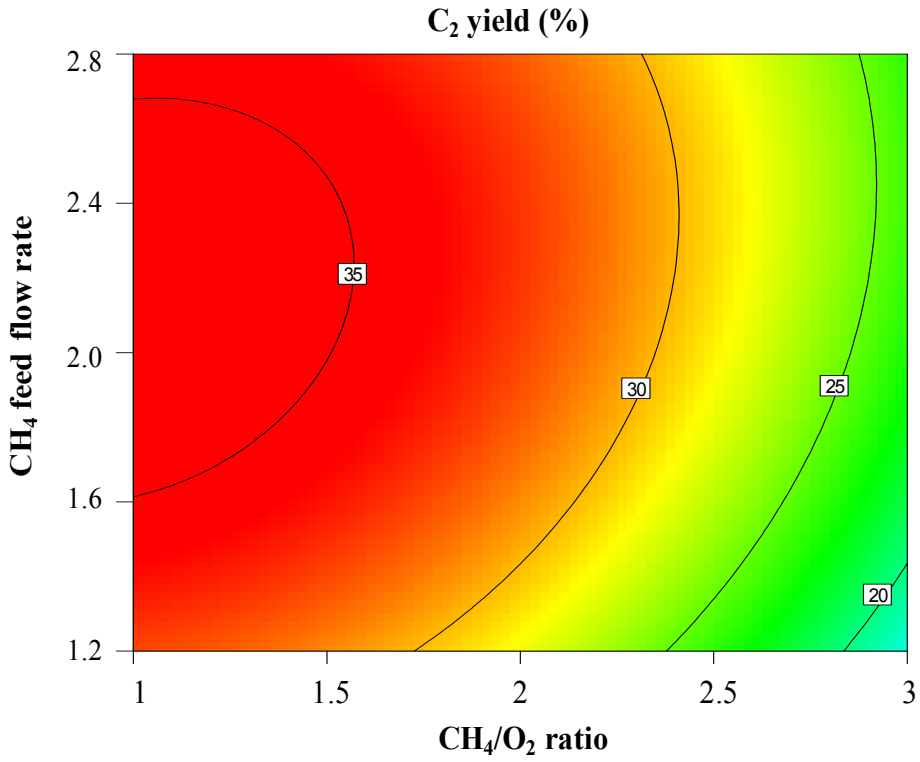

Figure 6.5 Contour surface plot of C_2 yield as a function of CH_4/O_2 ratio and CH_4 feed flow rate.

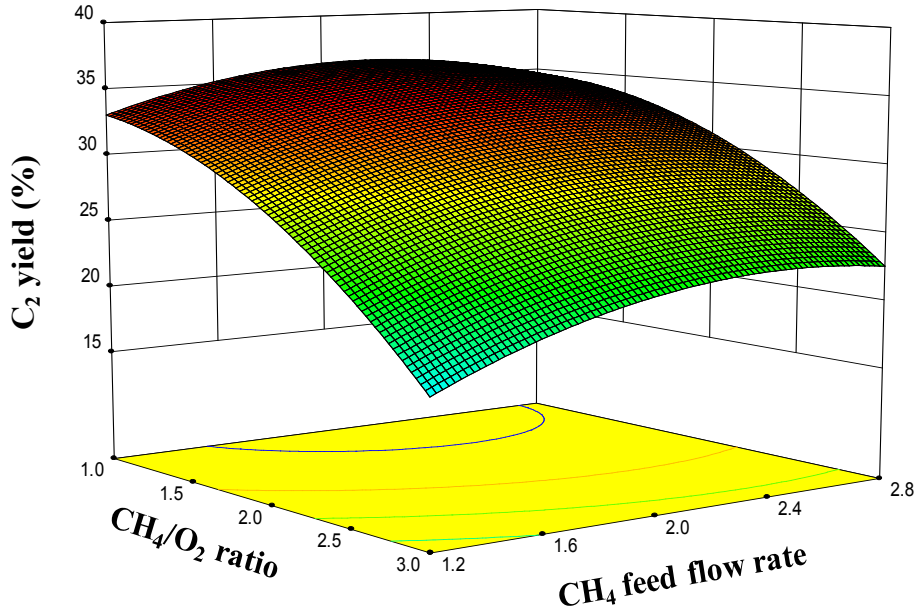

Figure 6.6 3-D graphic surface optimization of C_2 yield versus CH_4/O_2 ratio and CH_4 feed flow rate.

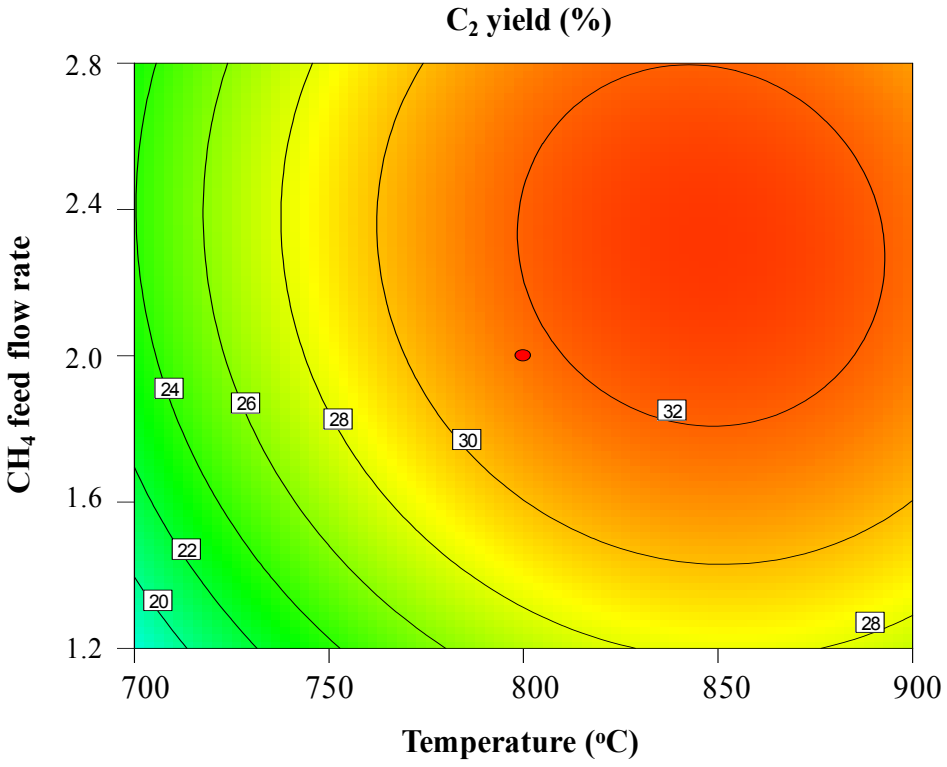

Figure 6.7 Contour surface plot of C_2 yield as a function of operating temperature and CH_4 feed flow rate.

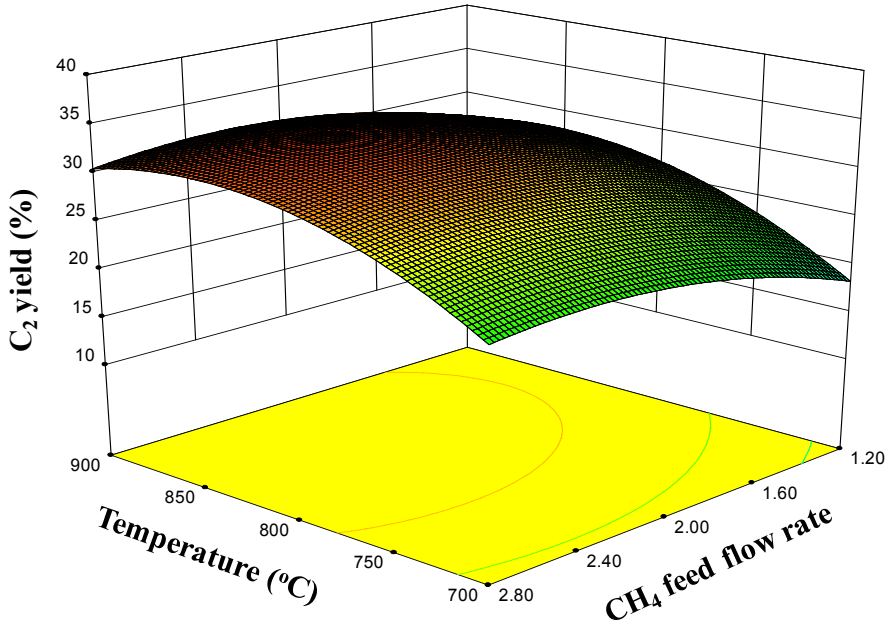

Figure 6.8 3-D graphic surface optimization of C_2 yield versus operating temperature and CH_4 feed flow rate.

6.2.3 Optimal operating parameters

In order to optimize the C_2 yield, the numerical feature of the DOE software was applied to find the optimum combination conditions that result in the maximum yield. It founds 9 solutions for the optimum conditions were generated and the solution with the highest desirability was selected to be verified by simulation method. Table 6.4 coupled with the predicted and simulated yield of C_2. From the table, the simulated optimum yield of 35.21% is well in agreement with the predicted value of 36.49%, with a relatively insignificant error of 3.64%. It can be concluded that the statistical model is useful in the accurate prediction and optimization of the OCM process.

Table 6.4 Comparison between simulation result and model prediction of the single-stage membrane for OCM process operated at the optimum conditions

Conditions	Optimum value	Predicted yield (%)	Simulated yield (%)	Error (%)
CH_4/O_2 ratio	0.83			
Temperature (°C)	847.44	36.49	35.21	3.64
CH_4 feed flow rate (10^{-3} mol/s)	2.10			

6.3 Optimization of multi-stage membrane reactor

According to Section 5.2.3, it can be seen that the proportion of oxygen at each stage as 50-30-20 (mol%) show a higher C_2 yield than the others. Thus, this section presents a study on determination of the optimal operating conditions for that oxygen feeding distribution case.

6.3.1 Regression model equation for C_2 yield

Simulations of a multi-stage membrane reactor for OCM process are performed based on the operating conditions as listed in Table 6.5. The results show that the C_2 yield is obtained varied from 15.28% to 38.91%, depending on the operating conditions. These results can be fitted by a second order quadratic model as given in Equation (6.4):

$$\begin{aligned} Y = & -321.286 + 20.344X_1 + 0.754X_2 + 17.785X_3 \\ & - 0.021X_1X_2 + 1.080X_1X_3 - (3.609\times10^{-3})X_2X_3 \\ & - 2.784X_1^2 - (4.094\times10^{-4})X_2^2 - 3.593X_3^2 \end{aligned} \tag{6.4}$$

From the equation, the yield of C_2 has linear and quadratic effects by the three process variables. This validation of the model obtained is shown by the R^2 error of 0.9866 or 98.66% of the response variability could be explained by this regression model. The value of R^2 is unity which means a complete agreement between predicted and actual responses. Figure 6.9 summarizes correlation between simulated values versus predicted values by using the developed model.

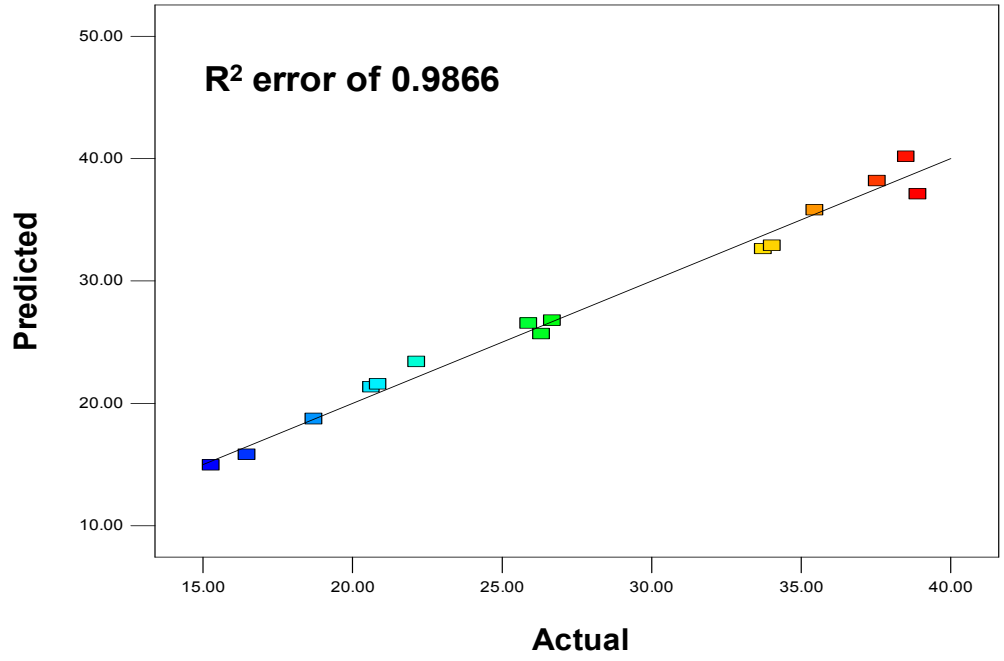

Figure 6.9 Predicted and actual values of C_2 yield for multi-stage membrane reactor.

Table 6.5 Full factorial central composite design matrix of three independent variables in coded and unit along with the simulated response value for a multi-stage membrane reactor (50-30-20).

Run	**Manipulated variables**						**Responses**
	X_1		X_2		X_3		C_2 yield (%)
	CH_4/O_2 ratio	Level	Temperature	Level	CH_4 feed flow rate	Level	
1	1	-1	700	-1	1.2	-1	22.15
2	1	-1	700	-1	2.8	1	25.90
3	1	-1	900	+1	1.2	-1	37.55
4	1	-1	900	+1	2.8	1	38.52
5	3	1	700	-1	1.2	-1	15.28
6	3	1	700	-1	2.8	1	20.86
7	3	1	900	+1	1.2	-1	20.64
8	3	1	900	+1	2.8	1	26.69
9	0.32	-α	800	0	2.0	0	38.91
10	3.68	+α	800	0	2.0	0	18.72
11	2	0	631.82	-α	2.0	0	16.48
12	2	0	968.18	+α	2.0	0	33.74
13	2	0	800	0	0.65	-α	26.33
14	2	0	800	0	3.35	+α	34.04
15	2	0	800	0	2.0	0	35.46

Statistical analysis based on ANOVA for the quadratic model developed by the software is shown in Table 6.6. The model F-value of 40.91 implies the model is significant. There is only a 0.04% chance that a "Model F-value" this large could occur due to noise. P-value less than 0.0500 indicate model terms are significant. In this case X_1, X_2, X_3, X_1X_2, X^2_1, X^2_2, X^2_3 are significant model terms. P-value greater than 0.1000 indicate the model terms are not significant.

Table 6.6 ANOVA of the response surface quadratic model for multi-stage membrane reactor.

Source	**SS**[a]	**DF**[b]	**MS**[c]	**F-value**	**Prof>F**
Model	956.82	9	106.31	40.91	0.0004
X_1	407.56	1	407.56	156.82	<0.0001
X_2	340.96	1	340.96	131.19	<0.0001
X_3	62.93	1	62.93	24.21	0.0044
X_1X_2	35.41	1	35.41	13.62	0.0141
X_1X_3	5.97	1	5.97	2.30	0.1901
X_2X_3	0.67	1	0.67	0.26	0.6340
X^2_1	46.92	1	46.92	18.05	0.0081
X^2_2	101.45	1	101.45	39.04	0.0015
X^2_3	32.01	1	32.01	12.32	0.0171
Residual	12.99	5	2.60		
Total	969.81	14			

[a] SS = Sum of squares, [b] DF = Degree of freedom, [c] MS = Mean square

Std. Dev.	1.61	R-Squared	0.9866
Mean	27.42	Adj R-Squared	0.9625
C.V. %	5.88	Pred R-Squared	0.1453
PRESS	828.92	Adeq Precision	19.154

The "Pred R-Squared" of 0.1453 is not as close to the "Adj R-Squared" of 0.9625 as one might normally expect. This may indicate a large block effect or a possible problem with this model and/or data. "Adeq Precision" measures the signal to noise ratio. A ratio greater than 4 is desirable. This ratio of 19.154 indicates an adequate signal. This model can be used to navigate the design space.

6.3.2 Results

6.3.2.1 Effect of one factor

The effect of CH_4/O_2 ratio, temperature and CH_4 feed flow rate on C_2 yield in case of a multi-stage membrane reactor as shown in Figure 6.10. The trend of the results from the regression model predictions are consistent with the results of the simulation studies in previous chapter. When considering the variable that can affect C_2 yield the most by comparing its p-value, CH_4/O_2 ratio and operating temperature are that variables due to the lowest p-value of <0.0001.

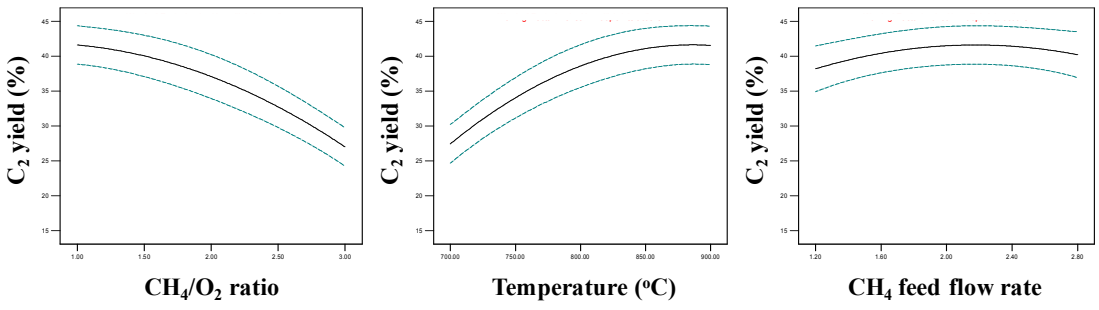

Figure 6.10 Effect of CH_4/O_2 ratio, temperature and CH_4 feed flow rate on C_2 yield in case of a multi-stage membrane reactor.

6.3.2.2 Effect of an interaction between two variables

Figures 6.11 and 6.12 demonstrate the contour surface plot and the response surface 3D plot indicating the effect of interaction between CH_4/O_2 ratio and operating temperature on C_2 yield, respectively. By analyzing the plots, the optimal

conditions obtained for C_2 yield were 1-2 of CH_4/O_2 ratio and the operating temperature of 800-900°C.

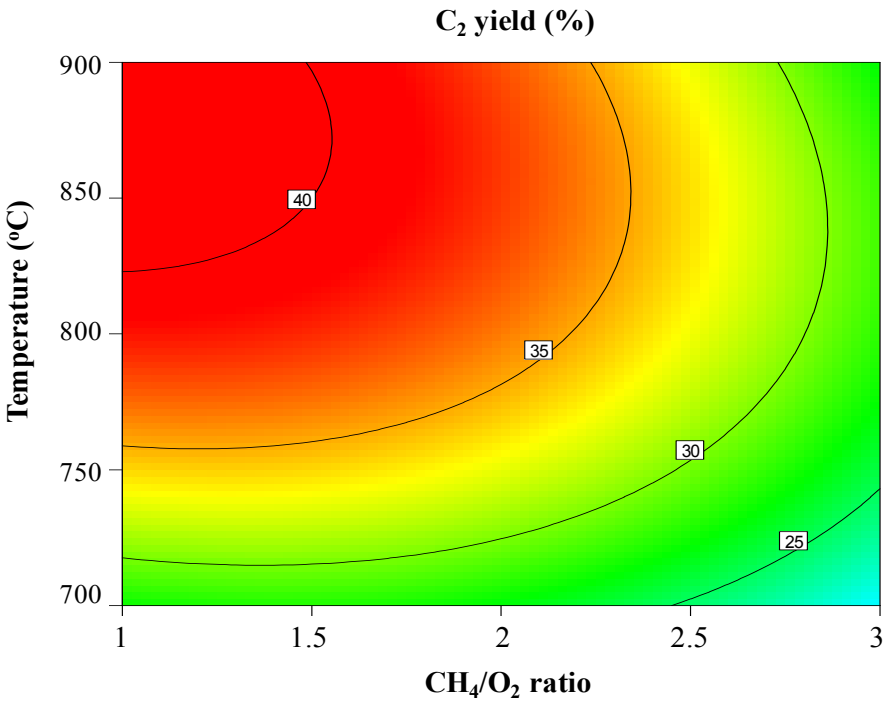

Figure 6.11 Contour surface plot of C_2 yield as a function of CH_4/O_2 ratio and operating temperature.

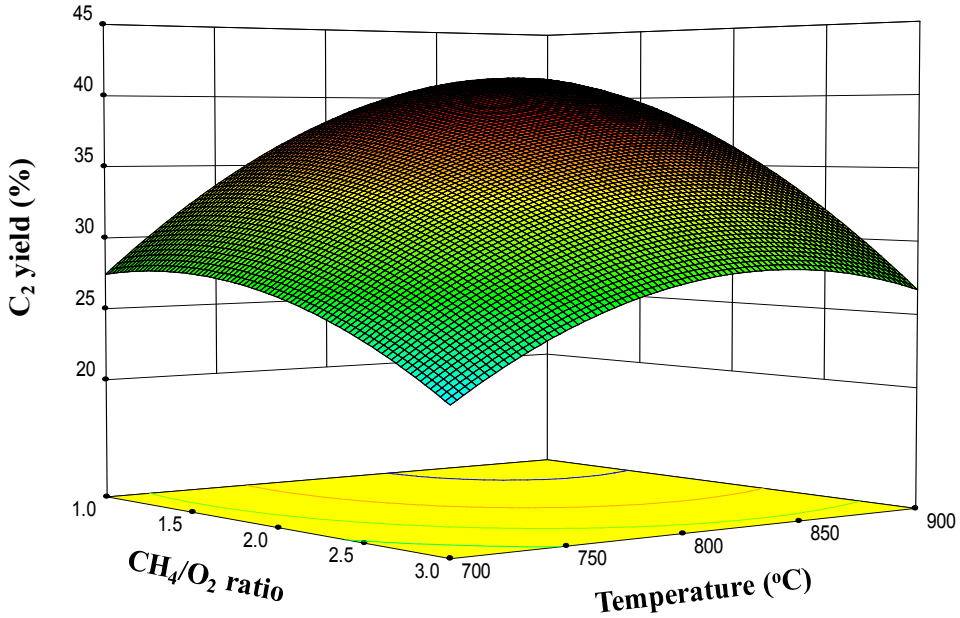

Figure 6.12 3-D graphic surface optimization of C_2 yield versus CH_4/O_2 ratio and operating temperature.

Figures 6.13 and 6.14 illustrate the contour surface plot and the response surface 3D plot indicating the effect of interaction between CH_4/O_2 ratio and CH_4 feed flow rate on C_2 yield, respectively. The optimum response value can be clearly observed from the contour plot. By analyzing the plots, the optimal conditions obtained for C_2 yield were 1-2 of CH_4/O_2 ratio and 1.5-2.8 (10^{-3} mol/s) of CH_4 feed flow rate.

Figures 6.15 and 6.16 present the contour surface plot and the response surface 3D plot indicating the effect of interaction between operating temperature and CH_4 feed flow rate on C_2 yield, respectively. By analyzing the plots, the optimal conditions obtained for C_2 yield were the operating temperature of 800-900°C and 1.5-2.8 (10^{-3} mol/s) of CH_4 feed flow rate.

When considering the interaction between two variables that can affect C_2 yield the most by comparing its p-value, the interaction between CH_4/O_2 ratio and operating temperature shows the most affect to C_2 yield due to the lowest p-value of 0.0141.

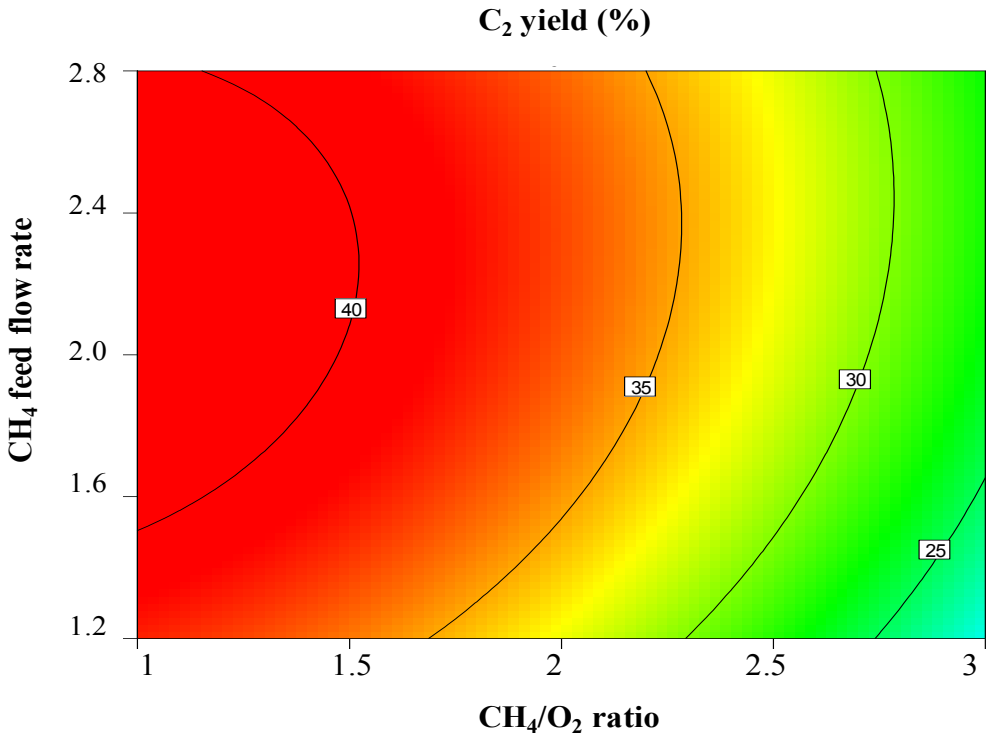

Figure 6.13 Contour surface plot of C_2 yield as a function of CH_4/O_2 ratio and CH_4 feed flow rate.

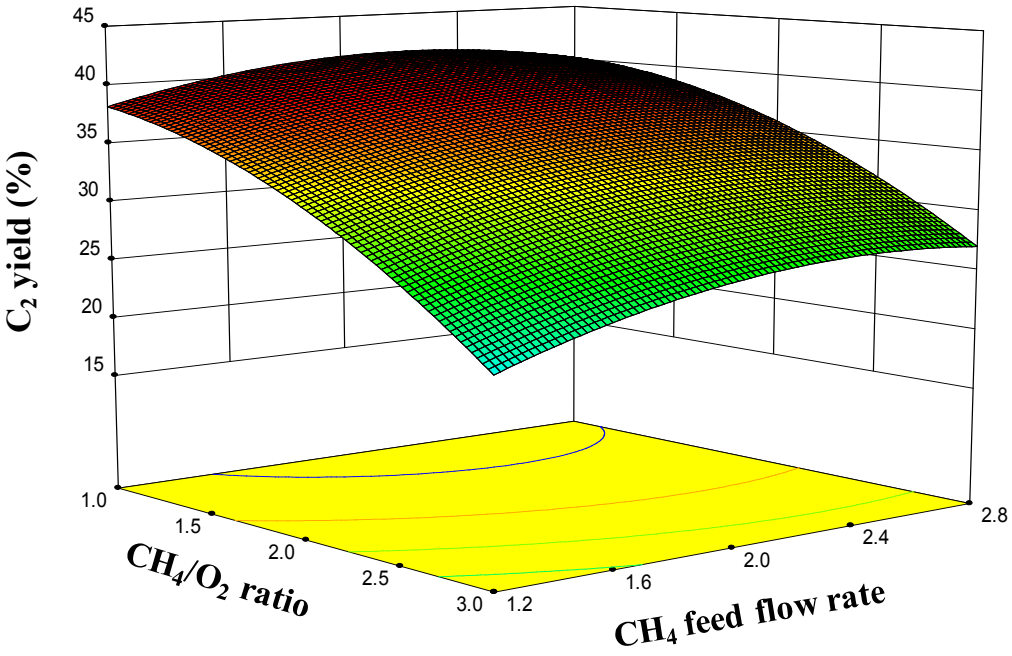

Figure 6.14 3-D graphic surface optimization of C_2 yield versus CH_4/O_2 ratio and CH_4 feed flow rate.

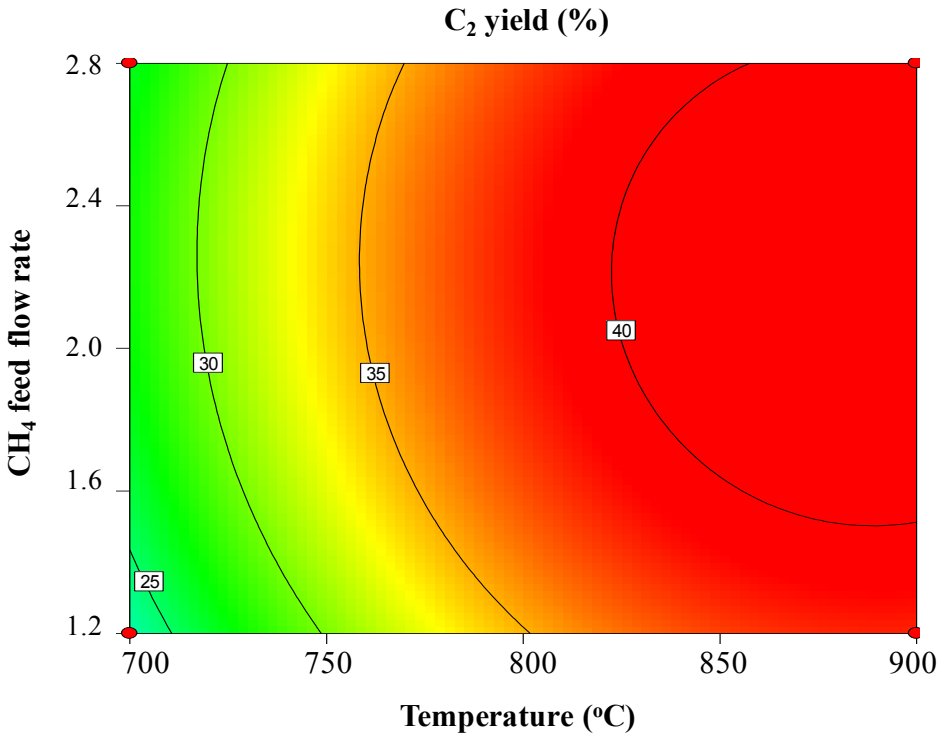

Figure 6.15 Contour surface plot of C_2 yield as a function of operating temperature and CH_4 feed flow rate.

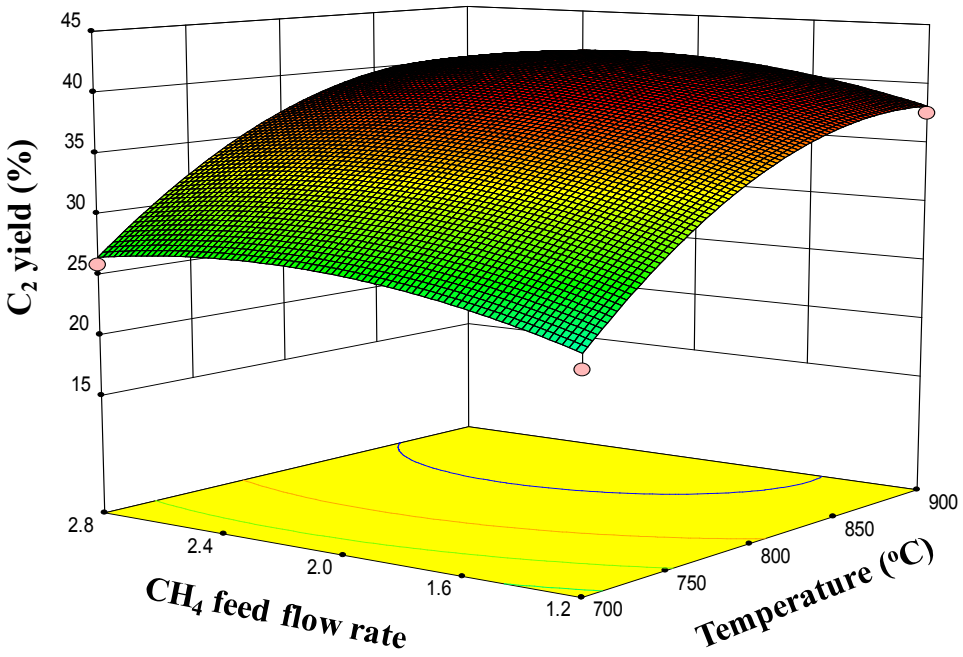

Figure 6.16 3-D graphic surface optimization of C_2 yield versus operating temperature and CH_4 feed flow rate.

6.3.3 Optimal operating parameters

In order to optimize the C_2 yield, the numerical feature of the DOE software was applied to find the optimum combination conditions that result in the maximum yield. It founds 11 solutions for the optimum conditions were generated and the solution with the highest desirability was selected to be verified by simulation method. Table 6.7 coupled with the predicted and simulated yield of C_2. From the table, the simulated optimum yield of 40.69% is well in agreement with the predicted value of 41.88%, with a relatively insignificant error of 2.92%. It can be concluded that the statistical model is useful in the accurate prediction and optimization of the OCM process.

Table 6.7 Comparison between simulation result and model prediction of the multi-stage membrane for OCM process operated at the optimum conditions.

Conditions	**Optimum value**	**Predicted yield (%)**	**Simulated yield (%)**	**Error (%)**
CH_4/O_2 ratio	0.69			
Temperature (°C)	849.21	41.88	40.69	2.92
CH_4 feed flow rate (10^{-3} mol/s)	2.13			

CHAPTER VII

CONCLUSION AND RECOMMENDATION

8.1 Conclusions

In this work, the performance of a dense tubular membrane reactor for oxidative coupling of methane (OCM) is investigated via simulation studies. The performance of reactor in terms of CH_4 conversion, C_2 selectivity and C_2 yield is considered with respect to the effect of key operating parameters, i.e., temperature, methane to oxygen feed ratio and methane feed flow rate. The first objective of this study is to analyze the performance of a single- and multi-stage membrane reactor for the OCM process. The results have shown that those operating parameters are sensitive parameters to the OCM reaction.

In a single stage membrane reactor, the membrane reactor considered consist of two concentric tubes: the outer tube is the shell; the inner tube is the dense $Ba_{0.5}Sr_{0.5}Co_{0.8}Fe_{0.2}O_{3-\delta}$ membrane. The methane is fed into the tube side of the reactor, while the oxygen is fed into the shell side. The La_2O_3/CaO catalyst is packed in the tube side. When the simulations are carried out with varying CH_4/O_2 ratio from 0.5 to 3, the operating temperature is constant at 800°C and methane feed flow rate is fixed at 1.6×10^{-3} mol/s, CH_4 conversion and C_2 yield decrease with increasing the CH_4/O_2 ratio and are highest at CH_4/O_2 ratio of 0.5 due to the higher oxygen concentration in the reaction side. C_2 selectivity decreases at higher CH_4 conversion and low CH_4/O_2 ratio is more suitable in terms of C_2 yield and C_2H_4/C_2H_6 ratio.

Initially, the CH_4 conversion and C_2 product yield increase with increasing operating temperature, but the C_2 product decreases as the temperature above 850 °C. The C_2 selectivity reduces with an increasing in temperature. The increasing of C_2H_4/C_2H_6 ratio with temperature suggests that the dehydrogenation of ethane to ethylene is favored at higher temperature. When varying CH_4 feed flow rate, the

methane conversion, C_2 selectivity and C_2 yield improve initially and reaching maximum values at the methane feed flow rate of 2×10^{-3} mol/s.

In a multi-stage membrane reactor, three arrangements of oxygen feeding distribution are considered, i.e., increased feed (10-30-60), uniform feed (33-33-33) and decreased feed (60-30-10). The total length of a three-stage membrane reactor is equal to a single stage one. The La_2O_3/CaO catalyst is packed in every stage of membrane reactors. The results have shown that the use of a multi-stage membrane reactor can improve the C_2 selectivity of the OCM process due to the controllable oxygen concentration in the reaction side. In addition, the multi-stage membrane reactor with a decreased oxygen feeding policy shows a better performance, in terms of C_2 selectivity and yield, compared with a conventional single-stage membrane reactor. This is because the adjustment of oxygen feed distributions at each membrane stage avoid the formation of high oxygen concentration zones.

The central composite design and the response surface method are effective to determine the optimum C_2 yield. It is found that the optimum conditions to maximize the C_2 production are estimated to be 847.44°C for the operating temperature, 2.10×10^{-3} mol/s for the CH_4 feed flow rate and the CH_4/O_2 ratio of 0.83 with the maximum C_2 yield of 36.49% and a relatively insignificant error of 3.64% for a single-stage membrane reactor. For a multi-stage membrane reactor with the proportion of oxygen at each stage as 50-30-20 (mol%), the optimum conditions to maximize the C_2 production are estimated to be 849.21°C for the operating temperature, 2.13×10^{-3} mol/s for the CH_4 feed flow rate and the CH_4/O_2 ratio of 0.69 with the maximum C_2 yield of 41.88% and a relatively insignificant error of 2.92%.

8.2 Recommendation

For a membrane reactor, since oxygen is permeated through a selective membrane, the effect of mass and heat transfer in a radial direction of this reactor should be investigated in more detail. The total pressure for both tube side and shell side in this study are constant at 1 atm. In order to know the performance of the OCM

process at different operating pressure, the effect of this parameter should be study as well.

REFERENCES

Alvarez-Galvan, M.C., Mota, N., Ojeda, M., Rojas, S., Navarro, R.M. and Fierro, J.L.G. Direct methane conversion routes to chemicals and fuels. Catalysis Today 171 (2011) : 15–23.

Amin, N.S. and Pheng, S.E. Influence of process variable and optimization of ethylene yield in oxidative coupling of methane over Li/MgO catalyst. Chemical Engineering Journal 116 (2006) : 187–197.

Baker, R.W. Membrane Technology and Applications. John Wiley, 2nd ed., 2004.

Bhatia, S., Thien, C.Y. and Mohamed, A.R. Oxidative coupling of methane (OCM) in a catalytic membrane reactor and comparison of its performance with other catalytic reactors. Chemical Engineering Journal 148 (2009) : 525‑532.

Bouwmeester, H.J.M. Dense ceramic membranes for methane conversion. Catalysis Today 82 (2003) : 141.

Ching, T.T., Abdul, R.M. and Subhash, B. Modeling of catalytic reactor for oxidative coupling of methane using La_2O_3/CaO catalyst. Chemical Engineering Journal 87 (2002) : 49–59.

Choudhary, V.R., Rane, V.H. and Pandit, Y.M. Comparison of alkali metal promoted mgo catalysts for their surface acidity basicity and catalytic activity selectivity in the oxidative coupling of methane. Journal Chemical Technology and Biotechnology 68 (1997) : 177-186.

Choudhary, V.R., Mulla, S.A.R., Pandit, M.Y., Chaudhari, S.T. and Rane, V.H. Influence of precursor of Li_2O and MgO on surface and catalytic properties of Li- promoted MgO in oxidative coupling of methane. Journal of Chemical Technology and Biotechnology 75 (2000) : 828-834.

Chua, Y.T., Mohamed, A.R. and Bhatia, S. Oxidative coupling of methane for the production of ethylene over sodium-tungsten-manganese-supported-silica catalyst(Na-W-Mn/SiO_2). Applied Catalysis A: General 343 (2008) : 142–148.

Cornell, J.A. How to apply response surface methodology. Vol. 8. American Society for Quality Control Statistics Division Winconsin : ASQS.

Couwenberg, P.M., Chen, Q. and Marin, G.B. Irreducible mass-transport limitations during a heterogeneously catalyzed gas-phase chain reaction: Oxidative coupling of methane. Industrial and Engineering Chemistry Research 35 (1996) : 415.

Daneshpayeh, M., Khodadi, A., Mostoufi, N., Mortazavi, Y., Gharebagh, R.S. and Talebizadeh, A. Kinetic modeling of oxidative coupling of methane over $Mn/Na_2WO_4/SiO_2$ catalyst. Fuel Processing Technology 90 (2009) : 403–410.

Djaidja, A., Barama, A. and Bettahar, M.M. Oxidative transformation of methane over nickel catalysts supported on rare-earth metal Oxides. Catalysis Today 61 (2000) : 303-307.

Driscoll, D.J., Martir, W., Wang, J.X. and Lunsford, J.H. Formation of gas phase methyl radicals over MgO. Journal of American Chemical Society 107 (1985) : 58-63.

Hong, J.H. and Yoon, K.J. Oxidative coupling of methane over calcium chlorine-promoted calcium chlorophosphate. Applied Catalysis A: General 205 (2001) : 253-262.

Hsieh, H.P. Inorganic Membranes for Separation and Reaction. Elsevier Science, 1996.

Huang, K., Zhan, X.L., Chen, F.Q., Lu, D.W. Catalyst design for methane oxidative coupling by using artificial neural network and hybrid genetic algorithm. Chemical Engineering Science 58 (2003) : 81.

Istadi and Amin, N.S. A hybrid numerical approach for multi responses optimization of process parameters and catalyst compositions in carbon dioxide oxidative coupling of methane over CaO–MnO/CeO_2 catalyst using response surface methodology. Fuel Processing Technology 87 (2006) : 49–459.

Ito, T., Wang, J.X., Lin, C.H. and Lunsford, J.H. Oxidative dimerization of methane Over a lithium-promoted magnesium oxide catalyst. Journal American Chemical Society 107 (1985) : 5062-5068.

James A. Carnell. MATLAB Applications in Chemical Engineering, 2003.

Ja˘so, S., Godini, H.R., Arellano-Garcia, H., Omidkhah, M. and Wozny, G. Analysis of attainable reactor performance for the oxidative methane coupling process. Chemical Engineering Science 65 (2010) : 6341‑6352.

Ji, S., Xiao, T., Li, S., Xu, C., Hou, R., Coleman, K.S. and Green, M.L.H. The relationship between the structure and the performance of Na-W-Mn/SiO_2 catalysis for the oxidative coupling of methane. Applied Catalysis A: General 225 (2002) : 271-284.

Kao, Y.K., Lei, L. and Lin, Y.S. Optimum operation of oxidative coupling of methane in porous ceramic membrane reactors. Catalysis Today 82 (2003) : 255–273.

Keller, G.E. and Bhasin, M.M. Synthesis of ethylene via oxidative coupling of methane. I. determination of active catalysts. Journal of Catalyst 73 (1982) : 9-19.

Kharton, V.V., Naumovich, E.N. and Nikolaev, A.V. Materials of high-temperature electrochemical oxygen membranes. Journal of Membrane Science 111 (1996) : 149.

Kiatkittipong, W., Goto, S., Tagawa, T., Assabumrungrat, S. and Praserthdam P. Simulation of oxidative coupling of methane in solid oxide fuel cell type reactor for C_2 hydrocarbon and electricity co-generation. Journal of Chemical Engineering of Japan 38 (2005) : 841–848.

Kim, S., Yang, Y.L., Jacobson, A.J. and Abeles, B. Diffusion and surface exchange coefficients in mixed ionic electronic conducting oxides from the pressure dependence of oxygen permeation. Solid State Ionics 106 (1998) : 189.

Kuo, J.C.W. Engineering evaluation of direct methane conversion process, In Wolf, E.E. (Ed.). Methane Conversion by Oxidative Processes. New York: Van Nostrand Reinhold (1992) : 486-526.

Kus, S., Otremba, M., Torz, A. and Taniewski, M. The effect of gas atmosphere used in the calcinations of MgO on its basicity and catalytic performance in oxidative coupling of methane. Applied Catalysis 230 (2002) : 263-270.

Lacombe, S., Durjanova, Z., Mleczko, L. and Mirodatos, C. Kinetic modelling of the oxidative coupling of methane over lanthanum oxide in connection with mechanistic studies. Chemical Engineering and Technology 18 (1995) : 216.

Lin, C.H., Wang, J.X. and Lunsford, J.H. Oxidative dimerization of methane over sodium-promoted calcium oxide. Journal of Catalysis 111 (1988) : 302-316.

Lu, Y., Dixon, A.G., Moser, W.R., Ma, Y.H., Balachandran, U. Oxygen-permeable dense membrane reactor for the oxidative coupling of methane. Journal of Membrane Science 170 (2000) : 27-44.

Liu, H., Wang, X., Yang, D., Gao, R., Wang, Z. and Yang, J. Scale up and stability test for oxidative coupling of methane over Na_2WO_4-Mn/SiO_2 catalyst in a 200 mL fixed-bed reactor. Journal of Natural Gas Chemistry 17 (2008) : 59-63.

Lunsford, J.H. and Driscoll, D.J. Gas-phase radical formation during the reaction of methane, ethane, ethylene and propylene over selected oxide catalysts. Journal of Physical Chemistry 89 (1985) : 4415-4418.

Lunsford, J.H., Catalytic conversion of methane to more useful chemicals and fuels: A challenge for the 21st Century, Catalysis Today 63 (2000) : 165-174.

Ma, C.C.M., C.T. Lee and H.D. Wu. Mechanical properties, thermal stability, and flame retardance of pultruded fiber-reinforced poly(ethylene oxide)-toughened novolak-type phenolic resin. Journal Applied Polymer Science, 68 (1998) : 1129-1136.

Mleczko L. and Baerns M. Catalytic oxidative coupling of methane-reaction engineering aspects and process schemes. Fuel Processing Technology 42 (1995) : 217–248.

Montgomery, L.D., Montgomery, R.W. and Guisado, R. Rheoencephalographic and electroencephalographic measures of cognitive workload: Analytical Procedures. Biological Psychology 40 (1995) : 143-159.

Mulder, M. Basic principles of membrane technology. Kluwer Academic Publishers, 1996.

Nouralishahi, A., Pahlavanzadeh, H. and Towfighi Daryan, J. Determination of optimal temperature profile in an OCM plug flow reactor for the maximizing of ethylene production. Fuel Processing Technology 89 (2008) : 667 – 677.

Oliver, L., Haag, S., Pennemann, H., Mirodatos, C. and Veen, A.C. van. Oxidative coupling of methane using catalyst modified dense perovskite membrane reactors. Catalysis Today 142 (2009) : 34‑41.

Olsbye, U., Desgrandchamps, G., Jens, K.J. and Kolboe, S. A kinetic study of the oxidative coupling of methane over a $BaCO_3$ / $La_2O_n(CO_3)_{3-n}$ catalyst. I. Determination of a global reaction scheme and the influence of heterogeneous and homogeneous reactions. Catalysis Today 13 (1992) : 209.

Omata, K., Hashimoto, S. Tominaga, H., Fujimoto, K. Oxidative coupling of methane using a membrane reactor. Applied Catalysis 51 (1989) : L1-L4.

Pak, S., Qiu, P. and Lunsford, J.H. Elementary reactions in the oxidative coupling of methane over $Mn/Na_2WO_4/SiO_2$ and $Mn/Na_2WO_4/MgO$ catalysts. Journal of Catalysis 179 (1998) : 222-230.

Pei, S., Kleefisch, M.S., Kobylinski, T.P., Faber, J., Udovich, C.A., Zhang-McCoy, V., Dabrowski, B., Balachandran, U., Mieville, R.L. and Poeppel, R.B. Failure mechanisms of ceramic membrane reactors in partial oxidation of methane to synthesis gas. Catalysis Letters 30 (1995) : 201.

Prodip, K., Kundu, Yan Zhang, Ajay K. Ray. Modeling and simulation of simulated countercurrent moving bed chromatographic reactor for oxidative coupling of methane. Chemical Engineering Science 64 (2009) : 5143 – 5152.

Sadeghzadeh Ahari, J., Ahmadi, R., Mikami, H., Inazu, K., Zarrinpashne, S., Suzuki, S. and Aika, K. Application of a simple kinetic model for the oxidative coupling of methane to the design of effective catalysts. Catalysis Today 145 (2009) : 45–54.

Sanchez Marcano, J.G. and Tsotsis, T.T. Catalytic membranes and membrane reactors. Wiley–VCH, 2002.

Shao, Z., Yang, W., Cong, Y., Dong, H., Tong, J. and Xiong, J. Investigation of the permeation behavior and stability of a $Ba_{0.5}Sr_{0.5}Co_{0.8}Fe_{0.2}O_{3-\delta}$ oxygen membrane. Membrane Science 172 (2000) : 177.

Sohrabi, M., Dabir, B., Eskandari A. and Golpasha, R.D. Some aspects of kinetics and mechanism of the oxidative coupling of methane. Journal of Chemical Technology and Biotechnology 67 (1996) : 15.

Stansch, Z., Mleczko, L. and Baerns, M. Comprehensive kinetics of oxidative coupling of methane over the La_2O_3/CaO catalyst. Industrial Engineering and Chemical Research 36 (1997) : 2568–2579.

Su, Y.S., Ying, J.K. and Green, W.H.J. Upper bound on the yield for oxidative coupling of methane. Journal of Catalysis 218 (2003) : 321–333.

Sun, J., Thybaut, J.W. and Marin, G.B. Microkinetics of methane oxidative coupling. Catalysis Today 137 (2008) : 90‑102.

Tjatjopoulos, G.J., Ketekides, P.T., Iatrides, D.K. and Vasalos, I.A. Cold flow model and computer simulation studies of a circulating fluidized bed reactor for the oxidative coupling of methane. Catalysis Today 21 (1994) : 387-399.

Tonkovich, A.L., Robert, W.C. and Rutherford, A. Enhanced C_2 yields form methane oxidative coupling by means of a separative chemical reactor. Science 262 (1993) : 221.

Traykova, M., Davidova, N., Tsaih, J.S. and Weiss, A.H. Oxidative coupling of methane - the transition from reaction to transport control over La_2O_3/MgO catalyst. Applied Catalysis A: General 169 (1998) : 237-247.

Trevor, D.J., Cox, D.M., Kaldor, A. and Am, J. Methane activation on unsupported platinum clusters. Chemical Society 112 (1990) : 3742–3749.

Wang, H., Cong Y., and Yang, W. Oxidative coupling of methane in $Ba_{0.5}Sr_{0.5}Co_{0.8}Fe_{0.2}O_3$ tubular membrane reactors. Catalysis Today 104 (2005) : 160–167.

Xin, Y., Song, Z., Tan, Y.Z. and Wang, D. The directed relation graph method for mechanism reduction in the oxidative coupling of methane. Catalysis Today 131 (2008) : 483–488.

Zeng, Y. and Lin, T.S. Oxidative coupling of methane on improved bismuth oxide membrane reactors. AIChe Journal 47.2 (2001a) : 436-444.

Zeng, Y. and Lin, T.S. Oxidative coupling of methane on fluorite-structured samarium-yttrium-bismuth oxide, Applied Catalysis A: General 213 (2001b) : 33-45.

Zheng, W., Cheng, D., Chen, F., Zhan, X. Characterization and catalytic behavior of Na-W-Mn-Zr-S-P/SiO_2 prepared by different methods in oxidative coupling of methane. Journal of Natural Gas Chemistry 19 (2010) : 515–521.

Zhu, X.F., Wang, H.H. and Yang, W.S. Novel cobalt-free oxygen permeable membrane. Chemical Communications 9 (2004) : 1130.

APPENDIX

APPENDIX A

LIST OF PUBLICATIONS

National conference

1. Sirikarn Tiraset, Wisitsree Wiyaratn, Suttichai Assabumrungrat and Amornchai Arpornwichanop. Simulation and optimization of oxidative coupling of methane in a dense tubular membrane reactor. (TIChE International Conference 2011, November 10-11, at Hatyai, Songkhla THAILAND).

VITA

Miss Sirikarn Tiraset was born in Suratthani on April 2, 1988. She received the Bachelor Degree in Chemical Engineering from Thammasat University in 2009. She began her graduate study in June 2010 when she entered the Graduate School of Chulalongkorn University and joined the Control and Systems Engineering group at the Department of Chemical Engineering.